Formation of millisecond pulsars I: Evolution of low-mass x-ray binaries with O_orb> 2days

Tauris, Th.M.; Savonije, G.J.

Publication date
1999

Published in
Astronomy & Astrophysics

Astron. Astrophys. 350, 928–944 (1999)

ASTRONOMY AND ASTROPHYSICS

Formation of millisecond pulsars

I. Evolution of low-mass X-ray binaries with $P_{\rm orb} > 2$ days

Thomas M. Tauris and Gerrit J. Savonije

Center for High-Energy Astrophysics, University of Amsterdam, Kruislaan 403, 1098 SJ Amsterdam, The Netherlands

Received 26 April 1999 / Accepted 6 August 1999

Abstract. We have performed detailed numerical calculations of the non-conservative evolution of close binary systems with low-mass (1.0–$2.0\,M_\odot$) donor stars and a $1.3\,M_\odot$ accreting neutron star. Rather than using analytical expressions for simple polytropes, we calculated the thermal response of the donor star to mass loss, in order to determine the stability and follow the evolution of the mass transfer. Tidal spin-orbit interactions and Reimers wind mass-loss were also taken into account.

We have re-calculated the correlation between orbital period and white dwarf mass in wide binary radio pulsar systems. Furthermore, we find an anti-correlation between orbital period and neutron star mass under the assumption of the "isotropic re-emission" model and compare this result with observations. We conclude that the accretion efficiency of neutron stars is rather low and that they eject a substantial fraction of the transferred material even when accreting at a sub-Eddington level.

The mass-transfer rate is a strongly increasing function of initial orbital period and donor star mass. For relatively close systems with light donors ($P_{\rm orb} < 10$ days and $M_2 < 1.3\,M_\odot$) the mass-transfer rate is sub-Eddington, whereas it can be highly super-Eddington by a factor of $\sim 10^4$ for wide systems with relatively heavy donor stars ($1.6 \sim 2.0\,M_\odot$) as a result of their deep convective envelopes. We briefly discuss the evolution of X-ray binaries with donor stars in excess of $2\,M_\odot$.

Based on our calculations we present evidence that PSR J1603–7202 evolved through a phase with unstable mass transfer from a relatively heavy donor star and therefore is likely to host a CO white dwarf companion.

Key words: stars: evolution – stars: mass-loss – stars: binaries: general – stars: neutron – stars: white dwarfs – methods: numerical

1. Introduction

Millisecond pulsars are characterized by short rotational periods ($P_{\rm spin} < 30$ ms) and relatively weak surface magnetic fields ($B < 10^{10}$ G) and are often found in binaries with a white dwarf companion. They are old neutron stars which have been recycled in a close binary via accretion of mass and angular momentum from a donor star. The general scenario of this process is fairly well understood qualitatively (cf. review by Bhattacharya & van den Heuvel 1991), but there remain many details which are still uncertain and difficult to analyze quantitatively. It is our aim to highlight these problems in a series of papers and try to answer them using detailed numerical calculations with refined stellar evolution and binary interactions.

There are now more than 30 binary millisecond pulsars known in the Galactic disk. They can be roughly divided into three observational classes (Tauris 1996). Class A contains the wide-orbit ($P_{\rm orb} > 20$ days) binary millisecond pulsars (BMSPs) with low-mass helium white dwarf companions ($M_{\rm WD} < 0.45\,M_\odot$), whereas the close-orbit BMSPs ($P_{\rm orb} \lesssim 15$ days) consist of systems with either low-mass helium white dwarf companions (class B) or systems with relatively heavy CO white dwarf companions (class C). The latter class evolved through a phase with significant loss of angular momentum (e.g. common envelope evolution) and descends from systems with a heavy donor star: $2 < M_2/M_\odot < 6$. The single millisecond pulsars are believed to originate from tight class B systems where the companion has been destroyed or evaporated – either from X-ray irradiation when the neutron star was accreting, or in the form of a pulsar radiation/wind of relativistic particles (e.g. Podsiadlowski 1991; Tavani 1992).

The evolution of a binary initially consisting of a neutron star and a main-sequence companion depends on the mass of the companion (donor) star and the initial orbital period of the system. If the donor star is heavy compared to the neutron star then the mass transfer is likely to result in a common envelope (CE) evolution (Paczynski 1976; Webbink 1984; Iben & Livio 1993) where the neutron star spirals in through the envelope of the donor in a very short timescale of less than 10^4 yr. The observational paucity of Roche-lobe filling companions more massive than $\sim 2\,M_\odot$ has been attributed to their inability to transfer mass in a stable mode such that the system becomes a persistent long-lived X-ray source (van den Heuvel 1975; Kalogera & Webbink 1996). For lighter donor stars ($< 2\,M_\odot$) the system evolves into a low-mass X-ray binary (LMXB) which evolves on a much longer timescale of 10^7–10^9 yr. It has been shown by Pylyser & Savonije (1988,1989) that an orbital bifurcation period ($P_{\rm bif}$) separates the formation of converging systems (which evolve with decreasing orbital periods until the mass-

Send offprint requests to: tauris@astro.uva.nl

losing component becomes degenerate and an ultra-compact binary is formed) from the diverging systems (which finally evolve with increasing orbital periods until the mass losing star has lost its envelope and a wide detached binary is formed). It is the LMXBs with $P_{\rm orb} > P_{\rm bif}$ ($\simeq 2$ days) which are the subject of this paper – the progenitors of the wide-orbit class A BMSPs.

In these systems the mass transfer is driven by the interior thermonuclear evolution of the companion star since it evolves into a (sub)giant before loss of orbital angular momentum dominates. In this case we get an LMXB with a giant donor. These systems have been studied by Webbink et al. (1983), Taam (1983), Savonije (1987), Joss et al. (1987) and recently Rappaport et al. (1995) and Ergma et al. (1998). For a donor star on the red giant branch (RGB) the growth in core-mass is directly related to the luminosity, as this luminosity is entirely generated by hydrogen shell burning. As such a star, with a small compact core surrounded by en extended convective envelope, is forced to move up the Hayashi track its luminosity increases strongly with only a fairly modest decrease in temperature. Hence one also finds a relationship between the giant's radius and the mass of its degenerate helium core – almost entirely independent of the mass present in the hydrogen-rich envelope (Refsdal & Weigert 1971; Webbink et al. 1983). In the scenario under consideration, the extended envelope of the giant is expected to fill its Roche-lobe until termination of the mass transfer. Since the Roche-lobe radius $R_{\rm L}$ only depends on the masses and separation between the two stars it is clear that the core-mass, from the moment the star begins Roche-lobe overflow, is uniquely correlated with the orbital period of the system. Thus also the final orbital period, $P_{\rm orb}^{\rm f}$ ($2 \sim 10^3$ days) is expected to be a function of the mass of the resulting white dwarf companion (Savonije 1987). It has also been argued that the core-mass determines the rate of mass transfer (Webbink et al. 1983). For a general overview of the evolution of LMXBs – see e.g. Verbunt (1990).

In this study we also discuss the final post-accretion mass of the neutron star and confront it with observations and the consequences of the new theory for kaon condensation in the core of neutron stars which result in a very soft equation-of-state and a corresponding maximum neutron star mass of only $\sim 1.5 M_\odot$ (Brown & Bethe 1994).

In Sect. 2 we briefly introduce the code, and in Sects. 3 and 4 we outline the orbital evolution and the stability criteria for mass transfer. We present the results of our LMXB calculations in Sect. 5 and in Sect. 6 we discuss our results and compare with observations. Our conclusions are given in Sect. 7 and a summary table of our numerical calculations is presented in the Appendix.

2. A brief introduction to the numerical computer code

We have used an updated version of the numerical stellar evolution code of Eggleton. This code uses a self-adaptive, non-Lagrangian mesh-spacing which is a function of local pressure, temperature, Lagrangian mass and radius. It treats both convective and semi-convective mixing as a diffusion process and finds a simultaneous and implicit solution of both the stellar structure equations and the diffusion equations for the chemical composition. New improvements are the inclusion of pressure ionization and Coulomb interactions in the equation-of-state, and the incorporation of recent opacity tables, nuclear reaction rates and neutrino loss rates. The most important recent updates of this code are described in Pols et al. (1995; 1998) and some are summarized in Han et al. (1994).

We performed such detailed numerical stellar evolution calculations in our work since they should result in more realistic results compared to models based on complete, composite or condensed polytropes.

We have included a number of binary interactions in this code in order to carefully follow the details of the mass-transfer process in LMXBs. These interactions include losses of orbital angular momentum due to mass loss, magnetic braking, gravitational wave radiation and the effects of tidal interactions and irradiation of the donor star by hard photons from the accreting neutron star.

3. The equations governing orbital evolution

The orbital angular momentum for a circular[1] binary is:

$$J_{\rm orb} = \frac{M_{\rm NS}\, M_2}{M}\, \Omega\, a^2 \tag{1}$$

where a is the separation between the stellar components, $M_{\rm NS}$ and M_2 are the masses of the (accreting) neutron star and the companion (donor) star, respectively, $M = M_{\rm NS} + M_2$ and the orbital angular velocity, $\Omega = \sqrt{GM/a^3}$. Here G is the constant of gravity. A simple logarithmic differentiation of this equation yields the rate of change in orbital separation:

$$\frac{\dot a}{a} = 2\frac{\dot J_{\rm orb}}{J_{\rm orb}} - 2\frac{\dot M_{\rm NS}}{M_{\rm NS}} - 2\frac{\dot M_2}{M_2} + \frac{\dot M_{\rm NS} + \dot M_2}{M} \tag{2}$$

where the total change in orbital angular momentum is:

$$\frac{\dot J_{\rm orb}}{J_{\rm orb}} = \frac{\dot J_{\rm gwr}}{J_{\rm orb}} + \frac{\dot J_{\rm mb}}{J_{\rm orb}} + \frac{\dot J_{\rm ls}}{J_{\rm orb}} + \frac{\dot J_{\rm ml}}{J_{\rm orb}} \tag{3}$$

The first term on the right side of this equation gives the change in orbital angular momentum due to gravitational wave radiation (Landau & Lifshitz 1958):

$$\frac{\dot J_{\rm gwr}}{J_{\rm orb}} = -\frac{32\, G^3}{5\, c^5}\frac{M_{\rm NS}\, M_2\, M}{a^4} \qquad {\rm s}^{-1} \tag{4}$$

where c is the speed of light in vacuum. The second term arises due to magnetic braking. This is is a combined effect of a magnetically coupled stellar wind and tidal spin-orbit coupling which tend to keep the donor star spinning synchronously with the orbital motion. Observations of low-mass dwarf stars with rotational periods in the range of $1 \sim 30$ days (Skumanich 1972) show that even a weak (solar-like) wind will slow down their rotation in the course of time due to interaction of the stellar wind

[1] We assume circular orbits throughout this paper – tidal effects acting on the near RLO giant star will circularize the orbit anyway on a short timescale of $\sim 10^4$ yr, cf. Verbunt & Phinney (1995).

with the magnetic field induced by the differential rotation in the convective envelope. For a star in a close binary system, the rotational braking is compensated by tidal coupling so that orbital angular momentum is converted into spin angular momentum and the binary orbit shrinks. Based on this observed braking law correlation between rotational period and age, Verbunt & Zwaan (1981) estimated the braking torque and we find:

$$\frac{\dot{J}_{\rm mb}}{J_{\rm orb}} \approx -0.5 \times 10^{-28}\, f_{\rm mb}^{-2}\, \frac{I R_2^2}{a^5}\, \frac{G M^2}{M_{\rm NS}\, M_2} \qquad {\rm s}^{-1} \tag{5}$$

where R_2 is the radius of the donor star, I is its moment of inertia and $f_{\rm mb}$ is a constant of order unity (see also discussion by Rappaport et al. 1983). In order to sustain a significant surface magnetic field we required a minimum depth of $Z_{\rm conv} > 0.065\, R_\odot$ for the convective envelope (cf. Pylyser & Savonije 1988 and references therein). Since the magnetic field is believed to be anchored in the underlaying radiative layers of the star (Parker 1955), we also required a maximum depth of the convection zone: $Z_{\rm conv}/R_2 < 0.80$ in order for the process of magnetic braking to operate. These limits imply that magnetic braking operates in low-mass ($M_2 \lesssim 1.5\, M_\odot$) stars which are not too evolved.

The third term on the right side of Eq. (3) describes possible exchange of angular momentum between the orbit and the donor star due to its expansion or contraction. For both this term and the magnetic braking term we estimate whether or not the tidal torque is sufficiently strong to keep the donor star synchronized with the orbit. The tidal torque is determined by considering the effect of turbulent viscosity in the convective envelope of the donor on the equilibrium tide. When the donor star approaches its Roche-lobe tidal effects become strong and lead to synchronous rotation. The corresponding tidal energy dissipation rate was calculated and taken into account in the local energy balance of the star. The tidal dissipation term was distributed through the convective envelope according to the local mixing-length approximation for turbulent convection – see Appendix for further details.

Since we present calculations here for systems with $P_{\rm orb} > 2$ days, the most significant contribution to the overall change in orbital angular momentum is caused by loss of mass from the system. This effect is given by:

$$\frac{\dot{J}_{\rm ml}}{J_{\rm orb}} \approx \frac{\alpha + \beta\, q^2 + \delta\, \gamma\, (1+q)^2}{1+q}\, \frac{\dot{M}_2}{M_2} \tag{6}$$

Here $q \equiv M_2/M_{\rm NS}$ is the mass ratio of the donor over the accretor and α, β and δ are the fractions of mass lost from the donor in the form of a fast wind, the mass ejected from the vicinity of the neutron star and from a circumstellar coplanar toroid (with radius, $a_{\rm r} = \gamma^2\, a$), respectively – see van den Heuvel (1994a) and Soberman et al. (1997). The accretion efficiency of the neutron star is thus given by: $\epsilon = 1 - \alpha - \beta - \delta$, or equivalently:

$$\partial M_{\rm NS} = -(1 - \alpha - \beta - \delta)\, \partial M_2 \tag{7}$$

where $\partial M_2 < 0$. Note, that these factors will also be functions of time as the binary evolve. Low-mass (1–2 $M_\odot$) donor stars do not lose any significant amount material in the form of a direct wind – except for an irradiated donor in a very close binary system, or an extended giant donor evolving toward the tip of the RGB which loses a significant amount of material in a wind. For the latter type of donors we used Reimers' (1975) formula to calculate the wind mass-loss rate:

$$\dot{M}_{2\,\rm wind} = -4 \times 10^{-13}\, \eta_{\rm RW}\, \frac{L\, R_2}{M_2} \qquad M_\odot\ {\rm yr}^{-1} \tag{8}$$

where the mass, radius and luminosity are in solar units and $\eta_{\rm RW}$ is the mass-loss parameter. We assumed $\eta_{\rm RW} = 0.5$ for our work – cf. Renzini (1981) and Sackmann et al. (1993) for discussions. The mass-loss mechanism involving a circumstellar toroid drains far too much orbital angular momentum from the LMXB and would be dynamical unstable resulting in a runaway event and formation of a CE. Also the existence of binary radio pulsars with orbital periods of several hundred days exclude this scenario as being dominant.

Hence, for most of the work in this paper we have $\alpha \ll \beta$, and we shall assume $\delta = 0$, and for LMXBs with large mass-transfer rates the mode of mass transfer to consider is therefore the "isotropic re-emission" model. In this model all of the matter flows over, in a conservative way, from the donor star to an accretion disk in the vicinity of the neutron star, and then a fraction, β of this material is ejected isotropically from the system with the specific orbital angular momentum of the neutron star.

As mentioned above, since we present calculations here for systems with initial periods larger than 2 days, loss of angular momentum due to gravitational wave radiation and magnetic braking (requiring orbital synchronization) will in general not be very significant.

3.1. The mass-transfer rate

For every timestep in the evolution calculation of the donor star the mass-transfer rate is calculated from the boundary condition on the stellar mass:

$$\dot{M}_2 = -1 \times 10^3\ PS \left[\ln \frac{R_2}{R_{\rm L}}\right]^3 \qquad M_\odot\ {\rm yr}^{-1} \tag{9}$$

where $PS[x] = 0.5\, [x + abs(x)]$ and $R_{\rm L}$ is the donor's Roche-radius given by (Eggleton 1983):

$$R_{\rm L} = \frac{0.49\, q^{2/3}\, a}{0.6\, q^{2/3} + \ln(1 + q^{1/3})} \tag{10}$$

The orbital separation a follows from the orbital angular momentum balance – see Eqs. (1) and (3). All these variables are included in a Henyey iteration scheme. The above expression for the mass-transfer rate is rather arbitrary, as is the precise amount of Roche-lobe overfill for a certain transfer rate; but the results are independent of the precise form as they are determined by the response of the stellar radius to mass loss.

4. Stability criteria for mass transfer

The stability and nature of the mass transfer is very important in binary stellar evolution. It depends on the response of the mass-losing donor star and of the Roche-lobe – see Soberman et al. (1997) for a nice review. If the mass transfer proceeds on a short timescale (thermal or dynamical) the system is unlikely to be observed during this short phase, whereas if the mass transfer proceeds on a nuclear timescale it is still able to sustain a high enough accretion rate onto the neutron star for the system to be observable as an LMXB for an appreciable interval of time.

When the donor evolves to fill its Roche-lobe (or alternatively, the binary shrinks sufficiently as a result of orbital angular momentum losses) the unbalanced pressure at the first Lagrangian point will initiate mass transfer (Roche-lobe overflow, RLO) onto the neutron star. When the donor star is perturbed by removal of some mass, it falls out of hydrostatic and thermal equilibrium. In the process of re-establishing equilibrium, the star will either grow or shrink – first on a dynamical (sound crossing), and then on a slower thermal (heat diffusion, or Kelvin-helmholtz) timescale. Also the Roche-lobe changes in response to the mass transfer/loss. As long as the donor star's Roche-lobe continues to enclose the star the mass transfer is stable. Otherwise it is unstable and proceeds on a dynamical timescale. Hence the question of stability is determined by a comparison of the exponents in power-law fits of radius to mass, $R \propto M^{\zeta}$, for the donor star and the Roche-lobe, respectively:

$$\zeta_{\rm donor} \equiv \frac{\partial \ln R_2}{\partial \ln M_2} \quad \wedge \quad \zeta_{\rm L} \equiv \frac{\partial \ln R_{\rm L}}{\partial \ln M_2} \tag{11}$$

where R_2 and M_2 refer to the mass losing donor star. Given $R_2 = R_{\rm L}$ (the condition at the onset of RLO) the initial stability criterion becomes:

$$\zeta_{\rm L} \leq \zeta_{\rm donor} \tag{12}$$

where $\zeta_{\rm donor}$ is the adiabatic or thermal (or somewhere in between) response of the donor star to mass loss. Note, that the stability might change during the mass-transfer phase so that initially stable systems become unstable, or vice versa, later in the evolution. The radius of the donor is a function of time and mass and thus:

$$\dot{R}_2 = \left.\frac{\partial R_2}{\partial t}\right|_{\rm M_2} + R_2\,\zeta_{\rm donor}\,\frac{\dot{M}_2}{M_2} \tag{13}$$

$$\dot{R}_{\rm L} = \left.\frac{\partial R_{\rm L}}{\partial t}\right|_{\rm M_2} + R_{\rm L}\,\zeta_{\rm L}\,\frac{\dot{M}_2}{M_2} \tag{14}$$

The second terms follow from Eq. (11); the first term of Eq. (13) is due to expansion of the donor star as a result of nuclear burning (e.g. shell hydrogen burning on the RGB) and the first term of Eq. (14) represents changes in $R_{\rm L}$ which are not caused by mass transfer such as orbital decay due to gravitational wave radiation and tidal spin-orbit coupling. Tidal coupling tries to synchronize the orbit whenever the rotation of the donor is perturbed (e.g. as a result of magnetic braking or an increase of the moment of inertia while the donor expands). The mass-loss rate of the donor can be found as a self-consistent solution to Eqs. (13) and (14) assuming $\dot{R}_2 = \dot{R}_{\rm L}$ for stable mass transfer.

4.1. The Roche-radius exponent, $\zeta_{\rm L}$

For binaries with orbital periods larger than a few days it is a good approximation that $\dot{J}_{\rm gwr}, \dot{J}_{\rm mb} \ll \dot{J}_{\rm ml}$ and $\alpha \ll \beta$ during the RLO mass-transfer phase. Assuming $\dot{J}_{\rm gwr} = \dot{J}_{\rm mb} = 0$ and $\alpha = \delta = 0$ we can therefore use the analytical expression obtained by Tauris (1996) for an integration of Eq. (2) to calculate the change in orbital separation during the LMXB phase (assuming a constant β):

$$\frac{a}{a_0} = \left(\frac{q_0\,(1-\beta)+1}{q\,(1-\beta)+1}\right)^{\frac{3\beta-5}{1-\beta}} \left(\frac{q_0+1}{q+1}\right) \left(\frac{q_0}{q}\right)^2 \Gamma_{\rm ls} \tag{15}$$

where the subscript '0' denotes initial values. Here we have added an extra factor, $\Gamma_{\rm ls}$:

$$\Gamma_{\rm ls} = \exp\left(2\int_0 \frac{(dJ)_{\rm ls}}{J_{\rm orb}}\right) \tag{16}$$

to account for the tidal spin-orbit coupling since $\dot{J}_{\rm ls} \neq 0$. One aim of this study is to evaluate the deviation of $\Gamma_{\rm ls}$ from unity.

If we combine Eqs. (7), (10) and (15), assuming $\Gamma_{\rm ls} = 1$, we obtain analytically:

$$\begin{aligned}\zeta_{\rm L} &= \frac{\partial \ln R_{\rm L}}{\partial \ln M_2} = \left(\frac{\partial \ln a}{\partial \ln q} + \frac{\partial \ln (R_{\rm L}/a)}{\partial \ln q}\right) \frac{\partial \ln q}{\partial \ln M_2} \\ &= [1 + (1-\beta)\,q]\,\psi + (5-3\beta)\,q \end{aligned} \tag{17}$$

where

$$\psi = \left[-\frac{4}{3} - \frac{q}{1+q} - \frac{2/5 + 1/3\,q^{-1/3}\,(1+q^{1/3})^{-1}}{0.6 + q^{-2/3}\ln(1+q^{1/3})}\right] \tag{18}$$

In the limiting case where $q \to 0$ (when the accretor is much heavier than the donor star) we find:

$$\lim_{q\to 0}\ \zeta_{\rm L} = -5/3 \tag{19}$$

The behavior of $\zeta_{\rm L}\,(q,\beta)$ for LMXBs is shown in Fig. 1. We note that $\zeta_{\rm L}$ does not depend strongly on β. This figure is quite useful to get an idea of the stability of a given mass transfer when comparing with ζ for the donor star. We see that in general the Roche-lobe, $R_{\rm L}$ increases ($\zeta_{\rm L} < 0$) when material is transferred from a light donor to a heavier NS ($q < 1$) and correspondingly $R_{\rm L}$ decreases ($\zeta_{\rm L} > 0$) when material is transferred from a heavier donor to a lighter NS ($q > 1$). This behavior is easily understood from the bottom panel of the same figure where we have plotted $-\partial \ln(a)/\partial \ln(q)$ as a function of q. The sign of this quantity is important since it tells whether the orbit expands or contracts in response to mass transfer (note $\partial q < 0$). We notice that the orbit always expands when $q < 1$ and it always decreases when $q > 1.28$, whereas for $1 < q \lesssim 1.28$ it can still expand if $\beta > 0$. There is a point at $q = 3/2$ where $\partial \ln(a)/\partial \ln(q) = 2/5$ is independent of β. It should be mentioned that if $\beta > 0$ then, in some cases, it is actually possible to decrease the separation, a between two stellar components while increasing $P_{\rm orb}$ at the same time!

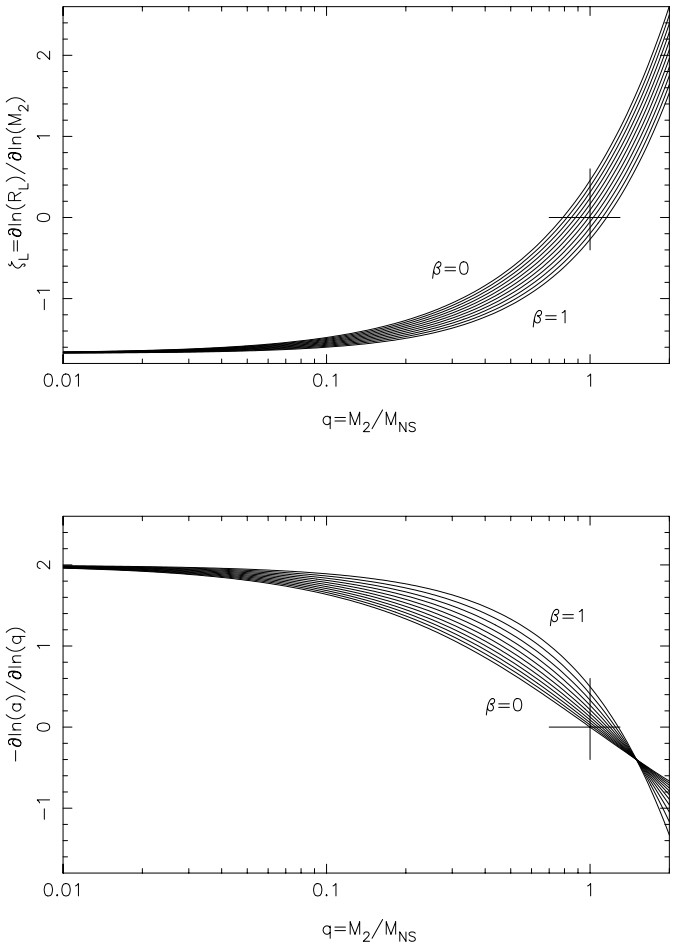

Fig. 1. Top panel: the Roche-radius exponent ($R_{\rm L} \propto M_2^{\zeta_{\rm L}}$) for LMXBs as a function of q and β. The different curves correspond to different constant values of β in steps of 0.1. Tidal effects were not taken into account ($\Gamma_{\rm ls} = 1$). A cross is shown to highlight the case of $q = 1$ or $\zeta_{\rm L} = 0$. In the bottom panel we have plotted $-\partial \ln(a)/\partial \ln(q)$ as a function of q. The evolution during the mass-transfer phase follows these curves from right to left (though β need not be constant) since M_2 and q are decreasing with time. See text for further explanation.

5. Results

We have evolved a total of a few hundred different LMXB systems. 121 of these are listed in Table A1 in the Appendix. We chose donor star masses of $1.0 \leq M_2/M_\odot \leq 2.0$ and initial orbital periods of $2.0 \lesssim P_{\rm orb}^{\rm ZAMS}/{\rm days} \leq 800$. We also evolved donors with different chemical compositions and mixing-length parameters. In all cases we assumed an initial neutron star mass of $1.3\,M_\odot$.

In Fig. 2 we show the evolution of four LMXBs. As a function of donor star mass (M_2) or its age since the ZAMS, we have plotted the orbital period ($P_{\rm orb}$), the mass-loss rate of the donor as well as the mass-loss rate from the system ($\dot{M}_2$ and $\dot{M}$), the radius exponent (ζ) of the donor and its Roche-lobe and finally the depth of the donor's convection zone ($Z_{\rm conv}/R_2$). Note, that we have zoomed in on the age interval which corresponds to the mass-transfer phase. As an example, we have chosen two different initial donor masses ($1.0\,M_\odot$ and $1.6\,M_\odot$) – each with two different initial orbital periods (3.0 and 60.0 days) of the neutron star (NS) and its ZAMS companion. The evolutionary tracks of the donor stars are plotted in the HR-diagram in Fig. 3. We will now discuss the evolution of each of these systems in more detail.

5.1. *Figure 2a*

In Fig. 2a we adopted $M_2^{\rm i} = 1.0\,M_\odot$ and $P_{\rm orb}^{\rm ZAMS} = 3.0$ days. In this case the time it takes for the donor to become a (sub)giant and fill its Roche-lobe, to initiate mass transfer, is 11.89 Gyr. Before the donor fills its Roche-lobe the expansion due to shell hydrogen burning causes its moment of inertia to increase which tends to slow down the rotation of the star. However, the tidal torques act to establish synchronization by transferring angular momentum to the donor star at the expense of orbital angular momentum. Hence at the onset of the mass transfer (A) the orbital period has decreased from the initial $P_{\rm orb}^{\rm ZAMS} = 3.0$ days to $P_{\rm orb}^{\rm RLO} = 1.0$ days and the radius is now $R_2 = R_{\rm L} = 2.0\,R_\odot$.

We notice that the mass-loss rate of the donor star remains sub-Eddington ($|\dot{M}_2| < \dot{M}_{\rm Edd} \approx 1.5 \times 10^{-8}\,M_\odot{\rm yr}^{-1}$ for hydrogen-rich matter) during the entire mass transfer[2]. Thus we expect all the transferred material to be accreted onto the neutron star, if disk instabilities and propeller effects can be neglected (see Sects. 5.7 and 6.4). Therefore we have no mass loss from the system in this case – i.e. $\dot{M} = 0$. The duration of the mass-transfer phase for this system is quite long: $\sim$1.0 Gyr (11.89 $\rightarrow$ 12.91 Gyr). At age, $t \sim 12.65$ Gyr ($P_{\rm orb} = 5.1$ days; $M_2 = 0.317\,M_\odot$) the donor star detaches slightly from its Roche-lobe (d) and the mass transfer ceases temporarily for $\sim$ 25 Myr – see next subsection for an explanation.

The Roche-radius exponent calculated from Eq. (17) is plotted as a dotted line as a function of M_2 in the upper right panel. However, our numerical calculations (full line) show that tidal effects are significant and increase ζ by $\sim$0.5–0.8 until $M_2 \approx 0.54\,M_\odot$ (p). At this point the magnetic braking is assumed to switch off, since $Z_{\rm conv}/R_2 > 0.80$. Note that during the mass transfer phase $\zeta \approx \zeta_{\rm L}$ and, as long as the mass transfer is not unstable on a dynamical timescale, we typically have in our code: $1 \times 10^{-4} < \ln(R_2/R_{\rm L}) < 7 \times 10^{-3}$ and hence practically $\zeta = \zeta_{\rm L}$.

The final outcome for this system is a BMSP with an orbital period of $P_{\rm orb}^{\rm f} = 9.98$ days and a He white dwarf (WD) with a mass of $M_{\rm WD} = 0.245\,M_\odot$ (B). The final mass of the NS is $M_{\rm NS} = 2.06\,M_\odot$, since we assumed all the material was accreted onto the NS given $|\dot{M}_2| < \dot{M}_{\rm Edd}$ during the entire X-ray phase. However, in Sect. 6 we will discuss this assumption

[2] Strictly speaking $\dot{M}_{\rm Edd} = \dot{M}_{\rm Edd}(R_{\rm NS})$ is slightly reduced during the accretion phase since the radius of the neutron star decreases with increasing mass (*e.g.* for an ideal n-gas polytrope: $R_{\rm NS} \propto M_{\rm NS}^{-1/3}$). However, this only amounts to a correction of less than 20% for various equations-of-state, and thus we have not taken this effect into account.

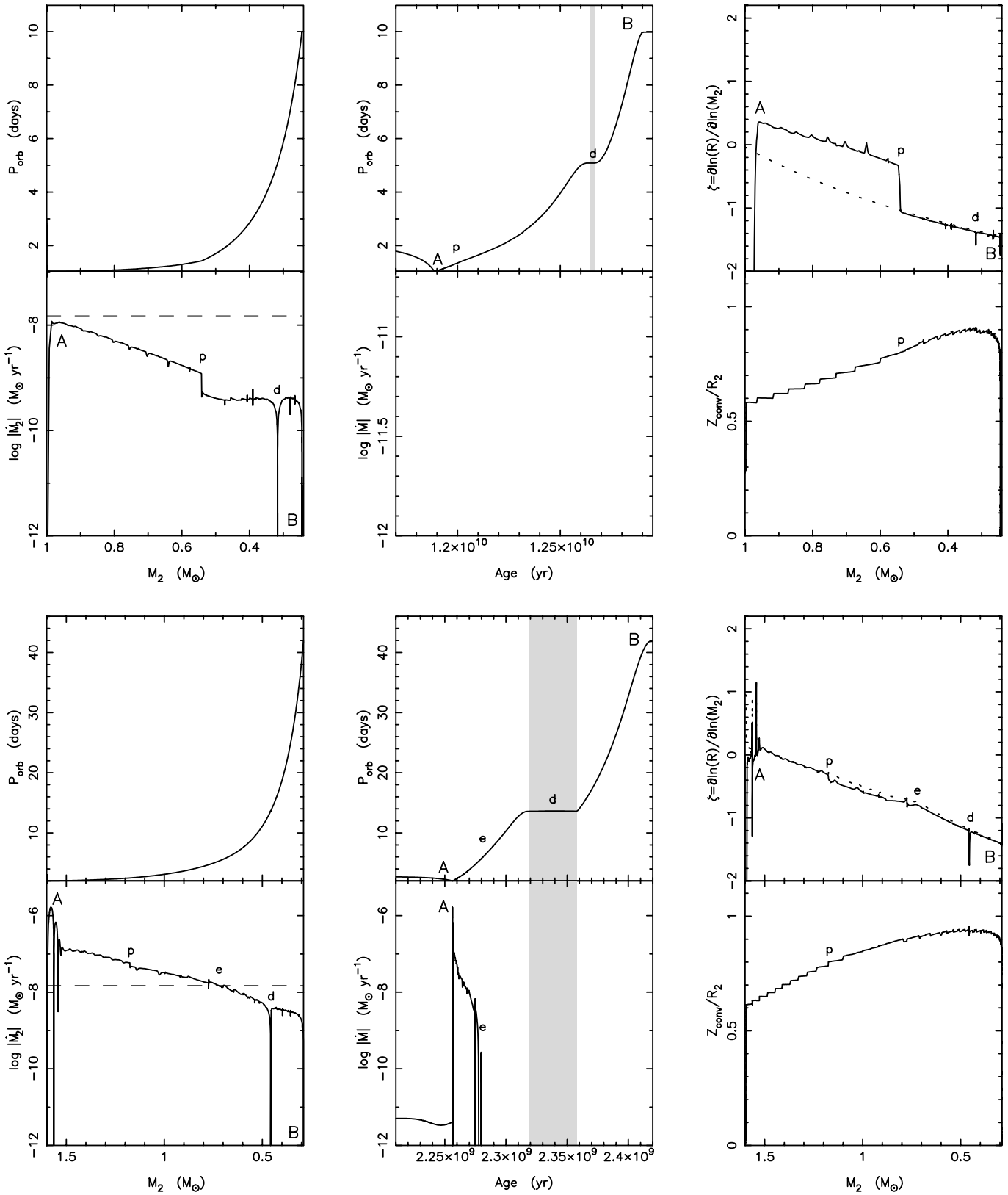

Fig. 2a and b. Numerical calculations of the mass-transfer process in two LMXB systems with $P_{\rm orb}^{\rm ZAMS} = 3.0$ days, $X = 0.70, Z = 0.02$ and $\alpha = 2.0$. The mass of the donor stars are **a**: $1.0\,M_{\odot}$, and **b**: $1.6\,M_{\odot}$ – top and bottom panels, respectively. See text for further details.

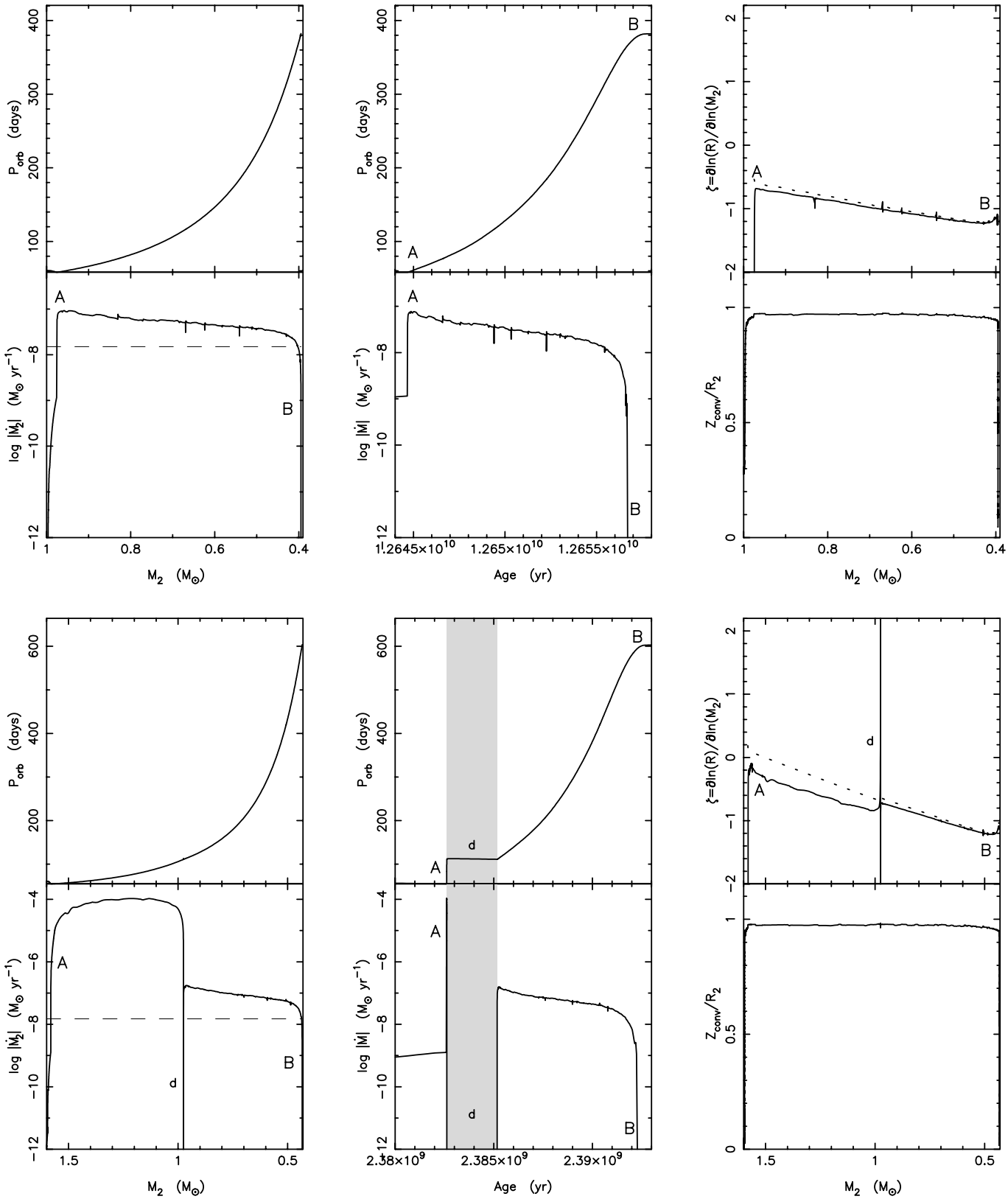

Fig. 2c and d. Numerical calculations of the mass-transfer process in two LMXB systems with $P_{\rm orb}^{\rm ZAMS} = 60.0$ days, $X = 0.70, Z = 0.02$ and $\alpha = 2.0$. The mass of the doner stars are **c**: $1.0\,M_{\odot}$, and **d**: $1.6\,M_{\odot}$ – top and bottom panels, respectively. See text for further details.

and the important question of disk instabilities and the propeller mechanism in more detail.

5.2. Figure 2b

In Fig. 2b we adopted $M_2^{\rm i} = 1.6\,M_\odot$ and $P_{\rm orb}^{\rm ZAMS} = 3.0$ days. The RLO is initiated at an age of $t = 2.256$ Gyr when $P_{\rm orb}^{\rm RLO} = 2.0$ days and $R_2 = 3.8\,R_\odot$ (A). In this case the mass-transfer rate is super-Eddington ($|\dot{M}_2| > \dot{M}_{\rm Edd}$, cf. dashed line) at the beginning of the mass-transfer phase. In our adopted model of "isotropic re-emission" we assume all material in excess of the Eddington accretion limit to be ejected from the system, while carrying with it the specific orbital angular momentum of the neutron star. Hence $|\dot{M}| = |\dot{M}_2| - \dot{M}_{\rm Edd}$. Initially $|\dot{M}_2| \approx 10^2 \dot{M}_{\rm Edd}$ at the onset of the RLO and then $|\dot{M}_2|$ decreases from 10 to $1\,\dot{M}_{\rm Edd}$ at $M_2 \approx 0.7 M_\odot$ (e) before it becomes sub-Eddington for the rest of the mass-transfer phase. Mass loss from the system as a result of a Reimers wind in the red giant stage prior to RLO (A) is seen to be less than $10^{-11}\,M_\odot\,{\rm yr}^{-1}$. By comparing the different panels for the evolution, we notice that the initial super-Eddington mass transfer phase ($A-e$) lasts for 22 Myr. In this interval the companion mass decreases from $1.6\,M_\odot$ to $0.72\,M_\odot$. Then the system enters a phase ($e-d$) of sub-Eddington mass transfer at $P_{\rm orb}$=5.31 days which lasts for 41 Myr. When $M_2 = 0.458\,M_\odot$, and $P_{\rm orb}$=13.6 days, the system detaches and the X-ray source is extinguished for about 40 Myr (d), cf. gray-shaded area. The temporary detachment is caused by a transient contraction of the donor star when its hydrogen shell source moves into the hydrogen rich layers left behind by the contracting convective core during the early main sequence stage. At the same time the convective envelope has penetrated inwards to its deepest point, i.e. almost, but not quite, to the H-shell source. The effect of a transient contraction of single low-mass stars evolving up the RGB, as a result of a sudden discontinuity in the chemical composition, has been known for many years (Thomas 1967; Kippenhahn & Weigert 1990) but has hitherto escaped attention in binary evolution. After the transient contraction the star re-expands enough to fill its Roche-lobe again and further ascends the giant branch. The corresponding final phase of mass transfer ($d-B$) is sub-Eddington ($|\dot{M}_2| \approx 0.2\,\dot{M}_{\rm Edd}$) and lasts for 60 Myr. The end product of this binary is a recycled pulsar and a He-WD companion with an orbital period of 41.8 days. In this case we obtain $M_{\rm WD} = 0.291\,M_\odot$ and $M_{\rm NS} = 2.05\,M_\odot$.

The total duration of the mass-transfer phase during which the system is an *active* X-ray source is $t_{\rm X} = 123$ Myr (excluding the quiescence phase of 40 Myr) which is substantially shorter compared to the case discussed above (Fig. 2a).

The reason for the relatively wide final orbit of this system, compared to the case discussed above with the $1.0\,M_\odot$ donor, is caused by the super-Eddington mass transfer during which a total of $0.55\,M_\odot$ is lost from the system.

The numerical calculations of ζ for this donor star (full line) fits very well with our simple analytical expression (dotted line) which indicates that the effects of the tidal spin-orbit interactions are not so significant in this case.

5.3. Figure 2c

In this figure we adopted $M_2^{\rm i} = 1.0\,M_\odot$ and $P_{\rm orb}^{\rm ZAMS} = 60.0$ days. The RLO is initiated (A) at an age of $t \simeq 12.645$ Gyr. At this stage the mass of the donor has decreased to $M_2^{\rm RLO} = 0.976\,M_\odot$ as a result of the radiation-driven wind of the giant star. However, the orbital period has also decreased ($P_{\rm orb}^{\rm RLO} = 58.1$ days) and thus the shrinking of the orbit due to tidal spin-orbit coupling dominates over the widening of the orbit caused by the wind mass loss.

The total interval of mass transfer is quite short, $t_{\rm X} = 13.3$ Myr. The mass-transfer rate is super-Eddington during the entire evolution ($|\dot{M}_2| \approx$ 1–6 $\dot{M}_{\rm Edd}$) and therefore the NS only accretes very little material: $\Delta M_{\rm NS} = \langle \dot{M}_{\rm Edd} \rangle\, \Delta t_{\rm mt} \approx 0.20\,M_\odot$. The reason for the high mass-loss rate of the donor star is its deep convective envelope (see lower right panel). Since the initial configuration of this system is a very wide orbit, the donor will be rather evolved on the RGB when it fills its Roche-lobe ($R_2 = 29.3\,R_\odot$ and $P_{\rm orb}^{\rm RLO} = 58.1$ days). Hence the donor swells up in response to mass loss (i.e. $\zeta < 0$) as a result of the super-adiabatic temperature gradient in its giant envelope. The radius exponent is well described by our analytical formula in this case. The final outcome of this system is a wide-orbit ($P_{\rm orb}^{\rm f} = 382$ days) BMSP with a $\sim 0.40\,M_\odot$ He-WD companion.

5.4. Figure 2d

Here we adopted $M_2^{\rm i} = 1.6\,M_\odot$ and $P_{\rm orb}^{\rm ZAMS} = 60.0$ days. At the onset of the RLO the donor mass is $M_2^{\rm RLO} = 1.582\,M_\odot$. In this case we do not only have a giant donor with a deep convective envelope. It is also (initially) heavier than the accreting NS. Both of these circumstances makes it difficult for the donor to retain itself inside its Roche-lobe once the mass transfer is initiated. It is likely that such systems, with huge mass-transfer rates, evolve into a phase where matter piles up around the neutron star and presumably forms a growing, bloated cloud engulfing it. The system could avoid a spiral-in when it manages to evaporate the bulk of the transferred matter from the surface of the (hot) accretion cloud via the liberated accretion energy. This scenario would require the radius of the accretion cloud, $r_{\rm cl}$ to be larger than $\sim R_{\rm NS}\,(|\dot{M}|/\dot{M}_{\rm Edd})$ in order for the liberated accretion energy to eject the transfered material. However, if there is insufficient gas cooling $r_{\rm cl}$ could be smaller from an energetic point of view. At the same time $r_{\rm cl}$ must be smaller than the Roche-lobe radius of the neutron star (cf. Eq. 10 with $q = M_{\rm NS}/M_2$) during the entire evolution. In that case our simple isotropic re-emission model would approximately remain valid. Assuming this to be the case we find the mass-transfer rate is extremely high: $|\dot{M}_2| \approx 10^4\,\dot{M}_{\rm Edd}$ and more than $0.5\,M_\odot$ is lost from the donor (and the system) in only a few 10^3 yr. The system survives and the orbital period increases from 54.5 days to 111 days during this short phase.

After this extremely short mass-transfer epoch, with an ultra-high mass-transfer rate, the donor star relaxes (d) and shrink inside its Roche-lobe for 2.5 Myr when $M_2 = 0.98\,M_\odot$.

The mass transfer is resumed again for 7.5 Myr at a more moderate super-Eddington rate ($d-B$). The final outcome is a binary pulsar with a $0.43\,M_\odot$ He-WD companion and an orbital period of 608 days. Though the NS only accretes $\sim 0.10\,M_\odot$ as a result of the short integrated accretion phase it will probably be spun-up sufficiently to become a millisecond pulsar since millisecond pulsars evidently are also formed in systems which evolve e.g. through a CE with similar (or even shorter) phases of accretion (van den Heuvel 1994b).

The initial extreme evolution of this system causes an offset in ζ until the more moderate mass-transfer phase ($d-B$) continues at $M_2 = 0.98\,M_\odot$. It should be noted that a system like this is very unlikely to be observed in the ultra-high mass-transfer state due to the very short interval ($< 10^4$ yr) of this phase.

5.5. $M_2 > 2\,M_\odot$, runaway mass transfer and onset of a CE

The latter example above illustrates very well the situation near the threshold for unstable mass transfer on a dynamical timescale and the onset of a CE evolution[3]. If the donor star is heavier than $1.8\,M_\odot$ a critical overflow is likely to occur since the orbit shrinks in response to mass transfer ($q < 1.28$, cf. Sect. 4). This is also the situation if $P_{\rm orb}$ is large because the donor in that case develops a deep convective envelope which causes it to expand in response to mass loss and a runaway mass transfer sets in. When a runaway mass transfer sets in we were not able to prevent it from critically overflowing its Roche-lobe and our code breaks down. At this stage the neutron star is eventually embedded in a CE with its companion and it will spiral in toward the center of its companion as a result of removal of orbital angular momentum by the drag force acting on it[4]. The final result of the CE depends mainly on the orbital period and the mass of the giant's envelope. If there is enough orbital energy available (i.e. if $P_{\rm orb}$ is large enough at the onset of the CE), then the entire envelope of the giant can be expelled as a result of the liberated orbital energy, which is converted into kinetic energy that provides an outward motion of the envelope decoupling it from its core. This leaves behind a tight binary with a heavy WD (the core of the giant) and a moderately recycled pulsar. There are five such systems observed in our Galaxy. They all have a CO-WD and $P_{\rm orb} = 6 \sim 8$ days. These are the so-called class C BMSPs.

If there is not enough orbital energy available to expel the envelope, then the NS spirals in completely to the center of the giant and a Thorne-Żytkow object is formed. Such an object might evolve into a single millisecond pulsar (e.g. van den Heuvel 1994a) or may collapse into a black hole (Chevalier 1996).

[3] We notice, that this very high mass-transfer rate might lead to hyper-critical accretion onto the neutron star and a possible collapse of the NS into a black hole if the equation-of-state is soft (cf. Chevalier 1993; Brown & Bethe 1994; Brown 1995). However, new results obtained by Chevalier (1996) including the centrifugal effects of a rotating infalling gas might change this conclusion.

[4] However, even binaries with donor stars of 2–6 $M_\odot$ might survive the mass transfer avoiding a spiral-in phase in case the envelope of the donor is still radiative at the onset of the RLO.

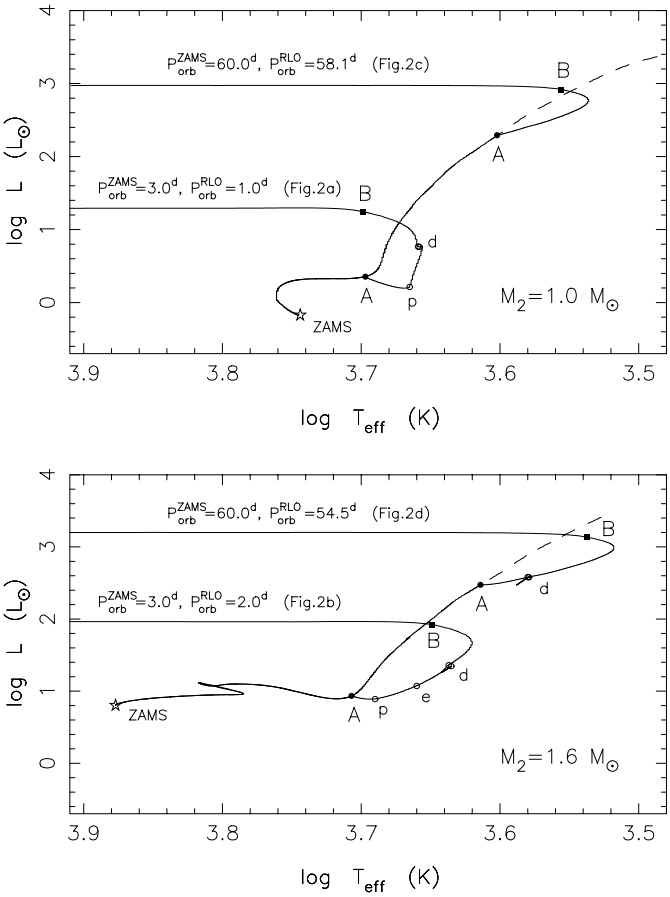

Fig. 3. Calculated evolutionary tracks in the Hertzsprung-Russel diagram of the four donor stars used in Fig. 2. The dashed lines represent the evolution of a single star with mass M_2. The mass-transfer phase (RLO) is initiated at A and ceases at B. The symbols along the evolutionary tracks correspond to those indicated in Fig. 2.

5.6. The ($P_{\rm orb}, M_{\rm WD}$) correlation

We have derived new ($P_{\rm orb}, M_{\rm WD}$) correlations based on the outcome of the 121 LMXB models calculated for this work. They are shown in Fig. 4a (the top panel). We considered models with donor star masses (M_2) in the interval 1.0–2.0 $M_\odot$, chemical compositions ranging from Population I (X=0.70, Z=0.02) to Population II (X=0.75, Z=0.001) and convective mixing-length parameters $\alpha \equiv l/H_{\rm p}$ from 2–3 (here l is the mixing length and $H_{\rm p}$ is the local pressure scaleheight). Following Rappaport et al. (1995) we chose our standard model with $M_2 = 1.0\,M_\odot$, Population I composition and $\alpha = 2$, cf. thick line in Fig. 4. The upper limit of M_2 is set by the requirement that the mass transfer in the binary must be dynamically stable, and the lower limit by the requirement that the donor star must evolve off the main sequence within an interval of time given by: $t_{\rm ms} < t_{\rm Hubble} - t_{\rm gal} - t_{\rm cool}$. Here $t_{\rm Hubble} \sim 15$ Gyr is the age of the Universe, $t_{\rm gal} \sim 1$ Gyr is the minimum time between the Big Bang and formation of our Milky Way and $t_{\rm cool} \sim 3$ Gyr is a typical low value of WD companion cooling ages, following the mass-transfer phase, as observed in BMSPs (Hansen & Phinney 1998). We thus find $M_2 \simeq 1.0\,M_\odot$ as a conservative lower limit.

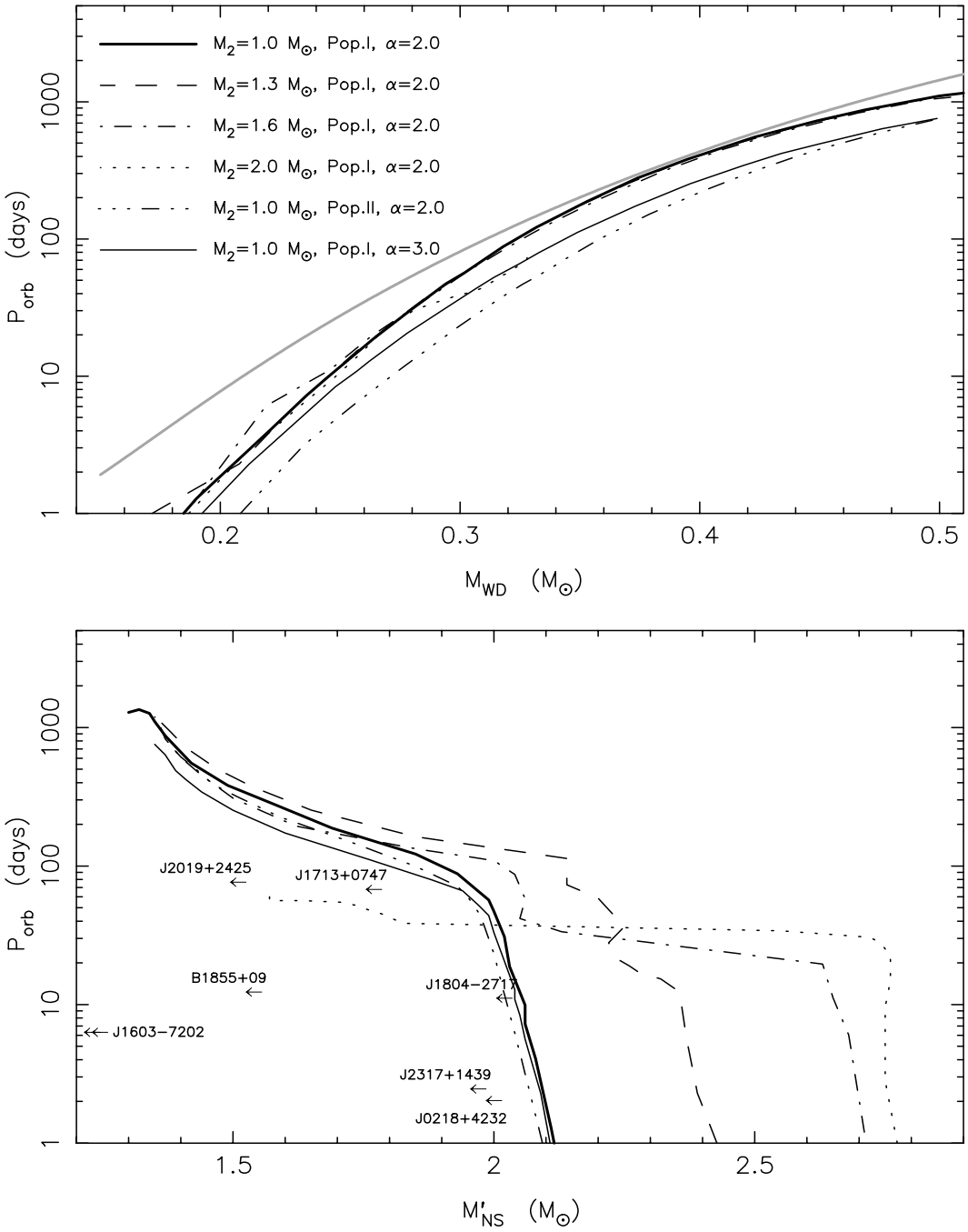

Fig. 4a and b. The ($P_{\rm orb}, M_{\rm WD}$) correlation (top panel) and the ($P_{\rm orb}, M_{\rm NS}$) anti-correlation (bottom panel) calculated for different donor star masses, M_2 chemical compositions (Pop.I: X=0.70; Z=0.02 and Pop.II: X=0.75; Z=0.001) and mixing-length parameters, α as indicated in the top panel. The gray line shows the correlation obtained by Rappaport et al. (1995) for $M_2 = 1.0\,M_\odot$, Pop.I chemical abundances and $\alpha = 2.0$. The post-accretion $M_{\rm NS}$ curves (bottom) assume no mass loss from accretion disk instabilities of propeller effects – see Sects. 5.7 and 6.4.

The first thing to notice, is that the correlation is more or less independent of the initial donor star mass (M_2) – only for $M_2 \gtrsim 2.0 M_\odot$ (where the mass transfer becomes dynamically unstable anyway for $P^{\rm i}_{\rm orb} \gtrsim 4.2$ days) we see a slight deviation. This result is expected if $M_{2\,\rm core}$ (and therefore R_2 and $P_{\rm orb}$) is independent of M_2. We have performed a check on this statement using our calculations for an evolved donor star on the RGB. As an example, in Table 1 we have written L, $T_{\rm eff}$ and $M_{2\,\rm core}$ as a function of M_2 when it has evolved to a radius of $50.0\,R_\odot$. In addition we have written the mass of the donor's envelope at the moment $R_2 = 50.0\,R_\odot$. We conclude, for a given chemical composition and mixing-length parameter, $M_{2\,\rm core}$ is practically independent of M_2 (to within a few per cent) and that mass loss from the envelope via RLO has similar little influence on the ($R_2, M_{2\,\rm core}$) correlation as well. For other choices of R_2 the differences were found to be smaller. In

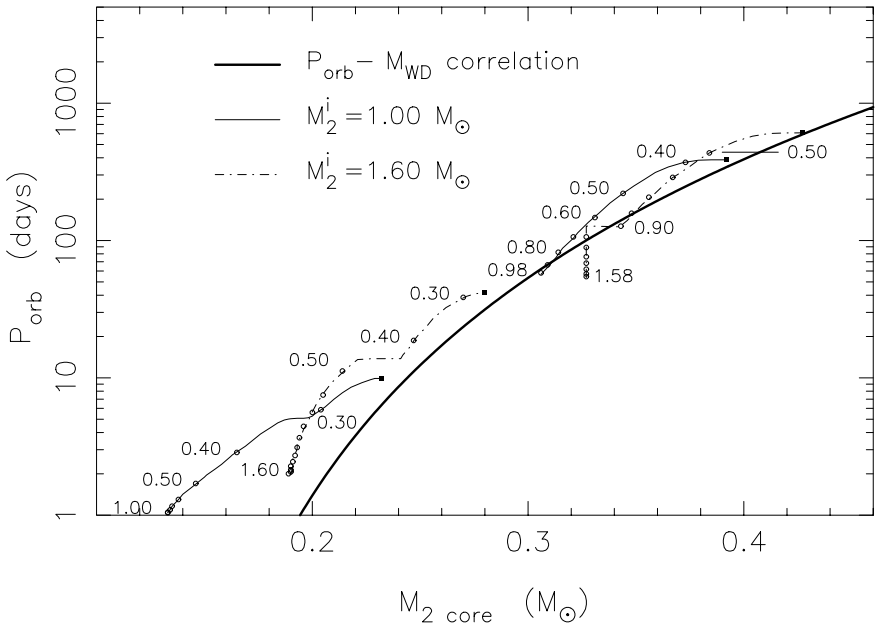

Fig. 5. Evolutionary tracks of the four LMXBs in Figs 2 and 3, showing the binary orbital period changing as a function of the mass of the core of the donor star. At the termination of the mass-transfer process $M_{2\,\mathrm{core}} \approx M_{\mathrm{WD}} - 0.01\,M_\odot$ and the end-points of the evolutionary tracks are located near the curve representing the $(P_{\mathrm{orb}}, M_{\mathrm{WD}})$ correlation. The initial orbital periods were $P_{\mathrm{orb}}^{\mathrm{ZAMS}} = 3.0$ days and $P_{\mathrm{orb}}^{\mathrm{ZAMS}} = 60.0$ days for the two bottom and top tracks, respectively. Furthermore we used Population I chemical abundances and $\alpha = 2$.

Table 1. Stellar parameters for a star with $R_2 = 50.0\,R_\odot$ – see text.

$M_2/M_\odot$	1.0**	1.6**	1.0*	1.6*
$\log L/L_\odot$	2.566	2.624	2.644	2.723
$\log T_{\mathrm{eff}}$	3.554	3.569	3.573	3.593
$M_{2\mathrm{core}}/M_\odot$	0.336	0.345	0.342	0.354
$M_{2\mathrm{env}}/M_\odot$	0.215	0.514	0.615	1.217

* Single star (X=0.70, Z=0.02 and α=2.0).
** Binary donor ($P_{\mathrm{orb}}^{\mathrm{ZAMS}} = 60.0$ days and $M_{\mathrm{NS}} = 1.3\,M_\odot$)

Fig. 5 we have shown P_{orb} (which resembles R_2) as a function of $M_{2\,\mathrm{core}}$.

Much more important is the theoretical uncertainty in the value of the convective mixing-length parameter and most important is the initial chemical composition of the donor star. We have estimated a $(P_{\mathrm{orb}}, M_{\mathrm{WD}})$ correlation from an overall best fit to all the models considered in Table A1 and obtain (P_{orb} in days):

$$\frac{M_{\mathrm{WD}}}{M_\odot} = \left(\frac{P_{\mathrm{orb}}}{b}\right)^{1/a} + c \qquad (20)$$

where, depending on the chemical composition of the donor,

$$(a,b,c) = \begin{cases} 4.50 & 1.2\times10^5 & 0.120 & \text{Pop.I} \\ 4.75 & 1.1\times10^5 & 0.115 & \text{Pop.I+II} \\ 5.00 & 1.0\times10^5 & 0.110 & \text{Pop.II} \end{cases} \qquad (21)$$

This formula is valid for binaries with: $0.18 \lesssim M_{\mathrm{WD}}^{\mathrm{He}}/M_\odot \lesssim 0.45$. The uncertainty in the initial chemical abundances of the donor star results in a spread of a factor $\sim$1.4 about the median (Pop.I+II) value of P_{orb} at any given value of M_{WD}. The spread in the $(P_{\mathrm{orb}}, M_{\mathrm{WD}})$ correlation arises solely from the spread in the $(R_2, M_{2\,\mathrm{core}})$ correlation as a result of the different chemical abundances, and/or α, of the giant donor star ascending the RGB.

If we compare our calculations with the work of Rappaport et al. (1995) we find that our best fit results in significantly lower values of P_{orb} for a given mass of the WD in the interval $0.18 \lesssim M_{\mathrm{WD}}/M_\odot \lesssim 0.35$. It is also notable that these authors find a maximum spread in P_{orb} of a factor $\sim$2.4 at fixed M_{WD}. For $0.35 \lesssim M_{\mathrm{WD}}/M_\odot \lesssim 0.45$ their results agree with our calculations to within 20 %. A fit to our Eq. (20) with the results of Rappaport et al. (1995) yields: $a = 5.75$, $b = 8.42\times10^4$ and $c = 0$ (to an accuracy within 1 % for $0.18 \lesssim M_{\mathrm{WD}}/M_\odot \lesssim 0.45$) for their donor models with population I chemical composition and $\alpha = 2.0$. For their Pop. II donors we obtain $b = 3.91\times10^4$ and same values for a and c as above. We also obtain somewhat lower values of P_{orb}, for a given mass of the WD, compared with the results of Ergma et al. (1998).

The discrepancy between the results of the above mentioned papers and our work is a result of different input physics for the stellar evolution (cf. Sect. 2). Ergma et al. (1998) uses models based on Paczynzki's code, and Rappaport et al. (1995) used an older version of Eggleton's code than the one used for this work. In our calculations we have also included the effects of tidal dissipation. However, these effects can not account for the discrepancy since in this paper we only considered binaries with $P_{\mathrm{orb}}^{\mathrm{i}} > 2$ days and thus the effects of the tidal forces are relatively small (the contribution to the stellar luminosity from dissipation of tidal energy is only $L_{\mathrm{tidal}} \lesssim 0.05 L_{\mathrm{nuc}}$ for $P_{\mathrm{orb}} = 2$ days).

In analogy with Rappaport et al. (1995) and Ergma et al. (1998) we find that, for a given value of M_{WD}, P_{orb} is decreasing with increasing α, and P_{orb} is increasing with increasing metallicity. We find $M_{\mathrm{WD}}^{z=0.001} \simeq M_{\mathrm{WD}}^{z=0.02} + 0.03 M_\odot$ which gives a stronger dependency on metallicity, by a factor $\sim$2, compared to the work of Ergma et al. (1998).

It should be noticed, that the $(P_{\mathrm{orb}}, M_{\mathrm{WD}})$ correlation is *independent* of β (the fraction of transferred material lost from the

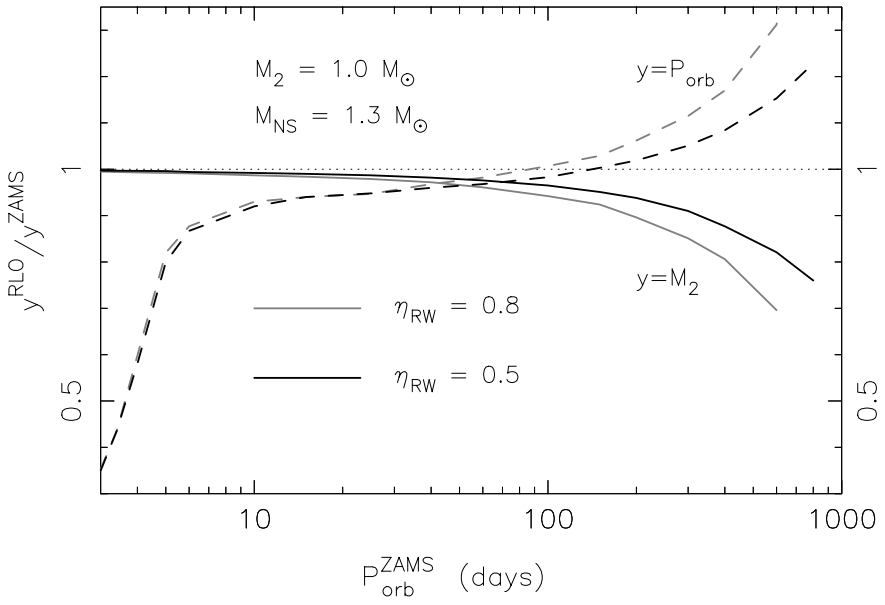

Fig. 6. The changes of donor mass, M_2 (full lines) and orbital period, $P_{\rm orb}$ (dashed lines), due to wind mass loss and tidal spin-orbit interactions, from the ZAMS until the onset of the RLO as a function of the initial orbital period. Plots are shown for two different values of the Reimers' mass-loss parameter, $\eta_{\rm RW}$. The binary is assumed to be circular. See text for further discussion.

system), the mode of mass loss and degree of magnetic braking since, as demonstrated above, the relationship between R_2 and $M_{2\,\rm core}$ of the giant donors remains unaffected by the exterior stellar conditions governing the process of mass transfer – see also Alberts et al. (1996). But for the *individual* binary, $P_{\rm orb}$ and $M_{\rm WD}$ do depend on β and they increase with increasing values of β (see e.g. the bottom panel of Fig. 1 for $q < 1$ which always applies near the end of the mass-transfer phase).

As mentioned in our examples earlier in this section, there is a competition between the wind mass loss and the tidal spin-orbit interactions for determining the orbital evolution prior to the RLO-phase. This is demonstrated in Fig. 6 where we have shown the changes in $P_{\rm orb}$ and M_2, from the ZAMS stage to the onset of the RLO, as a function of the initial ZAMS orbital period. It is seen that only for binaries with $P_{\rm orb}^{\rm ZAMS} > 100$ days will the wind mass-loss be efficient enough to widen the orbit. For shorter periods the effects of the spin-orbit interactions dominate (caused by expansion of the donor) and loss of orbital angular momentum causes the orbit to shrink.

5.7. The ($P_{\rm orb}, M_{\rm NS}$) anti-correlation

We now investigate the interesting relationship between the final mass of the NS and the final orbital period. In Fig. 4b (the bottom panel) we have plotted $P_{\rm orb}$ as a function of the potential maximum mass of the recycled pulsar, $M'_{\rm NS}$. This value is the final mass of the NS if mass loss resulting from instabilities in the accretion process are neglected. Another (smaller) effect which has also been ignored is the mass deficit of the accreted material as it falls deep down the gravitational potential well of the NS. The gravitational mass of a NS (as measured from a distant observer by its gravitational effects) contains not only the rest mass of the baryons, but also the mass equivalent of the negative binding energy, $\Delta M_{\rm def} = E_{\rm bind}/c^2 < 0$. Depending on the equation-of-state $\Delta M_{\rm def}$ ∼10% of the gravitational mass (Shapiro & Teukolsky 1983). This is hence also the efficiency of radiative emission in units of available rest-mass energy incident on the NS. Thus we can express the actual post-accretion gravitational mass of a recycled pulsar by ($\partial m_2 < 0$):

$$M_{\rm NS} = M_{\rm NS}^{\rm i} + \left[-\int_{M_2}^{M_{\rm WD}} (1-\beta')\,\partial m_2 - \Delta M_{\rm dp} \right] k_{\rm def} \quad (22)$$

Here $\beta' \equiv \max\left((|\dot{M}_2| - \dot{M}_{\rm Edd})/|\dot{M}_2|, 0 \right)$ is the fraction of material lost in a relativistic jet as a result of super-Eddington mass transfer; $\Delta M_{\rm dp} = \Delta M_{\rm disk} + \Delta M_{\rm prop}$ is the sum of matter lost from the accretion disk (as a result of viscous instabilities or wind corona) and matter being ejected near the pulsar magnetosphere as a result of the centrifugal propeller effect, and finally $k_{\rm def} = \langle \frac{M_{\rm NS}}{M_{\rm NS} - \Delta M_{\rm def}} \rangle \approx 0.90$ is a factor that expresses the ratio of gravitational mass to rest mass of the material accreted onto the NS. $M'_{\rm NS}$ used in Fig. 4b is given by the expression above assuming $\Delta M_{\rm dp} = 0$ and $\Delta M_{\rm def} = 0$ ($k_{\rm def} = 1$).

We see that the ($P_{\rm orb}, M'_{\rm NS}$) anti-correlation is more or less independent of the chemical composition and α of the donor star, whereas it depends strongly on M_2 for $P_{\rm orb} \lesssim 50$ days. This anti-correlation between $P_{\rm orb}$ and $M'_{\rm NS}$ is quite easy to understand: binaries with large initial orbital periods will have giant donor stars with deep convective envelopes at the onset of the mass transfer; hence the mass-transfer rate will be super-Eddington and subsequently a large fraction of the transferred material will be lost from the system. Therefore BMSPs with large values of $P_{\rm orb}$ are expected to have relatively light NS – cf. Sects. 5.3 (Fig. 2c) and 5.4 (Fig. 2d). Similarly, binaries with small values of $P_{\rm orb}^{\rm ZAMS}$ will result in BMSPs with relatively small $P_{\rm orb}$ and large values of $M'_{\rm NS}$, since $\dot{M}_2$ will be sub-Eddington and thus the NS has the potential to accrete all of the transferred material – cf. Sects. 5.1 (Fig. 2a) and 5.2 (Fig. 2b). Therefore, if disk instabilities, wind corona and propeller effects were unimportant we would expect to find an ($P_{\rm orb}, M_{\rm NS}$) anti-correlation among the observed BMSPs. However, below (Sect. 6.2) we demonstrate that mass ejection arising from these

effects is indeed important and thus it is very doubtful whether an $(P_{\rm orb}, M_{\rm NS})$ anti-correlation will be found from future observations.

6. Discussion and comparison with observations

6.1. Comparison with condensed polytrope donor models

Hjellming & Webbink (1987) studied the adiabatic properties of three simple families of polytropes by integrating the non-linear Lane-Emden equation in Lagrangian coordinates. The condensed polytropes, consisting of $n = 3/2, \gamma = 5/3$ (convective) envelopes with He-core point masses, are suitable for red giant stars. In is not trivial to directly compare our calculations with e.g. the stability analysis of Soberman et al. (1997) and Kalogera & Webbink (1996) since the donor does not restore (thermal) equilibrium after initiation of an unstable mass-transfer process. But it is important to point out, that systems which initiate RLO with thermally unstable mass transfer could, in some cases, survive this temporary phase – even if $|\dot{M}_2|$ exceeds the Eddington accretion limit by as much as a factor $\sim 10^4$ (see Fig. 2d). Similarly, systems which begin mass transfer on a thermal timescale may in some cases (if M_2 is large compared to $M_{\rm NS}$) eventually become dynamically unstable. These results were also found by Hjellming (1989) and Kalogera & Webbink (1996), and we refer to these papers for a more detailed discussion on the fate of thermally unstable systems. Therefore it is not always easy to predict the final outcome of an LMXB system given its initial parameters – especially since the onset criteria of a CE phase is rather uncertain. Nevertheless, we can conclude that LMXBs with $M_2 \leq 1.8\,M_\odot$ will always survive the mass transfer phase. Systems with donor stars $M_2 \geq 2\,M_\odot$ only survive if $P_{\rm orb}^{\rm ZAMS}$ is within a certain interval.

Soberman et al. (1997) also used the polytropic models of Hjellming & Webbink (1987) to follow the mass transfer in binaries. The global outcome of such calculations are reasonably good. However, the weakness of the polytropic models is that whereas they yield the radius-exponent at the onset of the mass transfer, and the approximated stellar structure at that given moment, they do not trace the response of the donor very well during the mass-transfer phase. The structural changes of the donor star (e.g. the outward moving H-shell and the inward moving convection zone giving rise to the transient detachment of the donor from its Roche-lobe) can only be followed in detail by a Henyey-type iteration scheme for a full stellar evolutionary model.

6.2. The observed ($P_{\rm orb}, M_{\rm WD}$) correlation

The companion mass, $M_{\rm WD}$ of an observed binary pulsar is constrained from its Keplerian mass function which is obtained from the observables $P_{\rm orb}$ and $a_{\rm p} \sin i$:

$$f\,(M_{\rm NS}, M_{\rm WD}) = \frac{(M_{\rm WD}\ \sin i)^3}{(M_{\rm NS}+M_{\rm WD})^2} = \frac{4\pi^2}{G}\ \frac{(a_{\rm p}\sin i)^3}{P_{\rm orb}^2} \quad (23)$$

Here i is the inclination angle (between the orbital angular momentum vector and the line-of-sight toward the observer) and $a_{\rm p} = a\,(M_{\rm WD}/(M_{\rm NS}+M_{\rm WD}))$ is the semi-major axis of the pulsar in a c.m. reference frame. The probability of observing a binary system at an inclination angle i, less than some value i_0, is $P(i<i_0) = 1-\cos(i_0)$.

As mentioned earlier, there are indeed problems with fitting the observed low-mass binary pulsars onto a theoretical core-mass period relation. The problem is particularly pronounced for the very wide-orbit BMSPs. Although the estimated masses of the companions are quite uncertain (because of the unknown orbital inclination angles and $M_{\rm NS}$) no clear observed $(P_{\rm orb}, M_{\rm WD})$ correlation seems to be present – opposite to what is proposed by several authors (e.g. Phinney & Kulkarni 1994, Lorimer et al. 1996 and Rappaport et al. 1995). In Table A2 in the Appendix we have listed all the observed galactic (NS+WD) binary pulsars and their relevant parameters. It was noticed by Tauris (1996) that the five BMSPs with $P_{\rm orb} > 100$ days all seem to have an observed $M_{\rm WD}^{\rm obs}$ which is lighter than expected from the theoretical correlation (at the $\sim$80 % confidence level on average). There does not seem to be any observational selection effects which can account for this discrepancy (Tauris 1996; 1998) – *i.e.* why we should preferentially observe systems with small inclination angles (systematic small values of i, rather than a random distribution, would increase $M_{\rm WD}^{\rm obs}$ for the given observed mass functions and thus the observations would match the theory). Evaporation of the companion star, from a wind of relativistic particles after the pulsar turns on, also seems unlikely since the evaporation timescale (proportional to $P_{\rm orb}^{4/3}$) becomes larger than $t_{\rm Hubble}$ for such wide orbits. It is also worth mentioning that the orbital period change due to evaporation, or general mass-loss in the form of a stellar wind, is at most a factor of $\sim$2, if one assumes the specific angular momentum of the lost matter is equal to that of the donor star.

Beware that the $(P_{\rm orb}, M_{\rm WD})$ correlation is *not* valid for BMSPs with CO/O-Ne-Mg WD companions as these systems did not evolve through a phase with stable mass transfer. The exception here are the very wide orbit systems with $P_{\rm orb}^{\rm f} \gtrsim 800$ days. PSR B0820+02 might be an example of such a system. From Table A1 (Appendix) it is seen that we expect a maximum orbital period of ~ 1400 days for the NS+WD binaries. Larger periods are, of course, possible but the binaries are then too wide for the neutron star to be recycled via accretion of matter.

It should also be mentioned that the recycling process is expected to align the spin axis of the neutron star with the orbital angular momentum vector as a result of $> 10^7$ yr of stable disk accretion. Hence we expect (Tauris 1998) the orbital inclination angle, i to be equivalent to (on average) the magnetic inclination angle, $\alpha_{\rm mag}$ defined as the angle between the pulsar spin axis and the center of the pulsar beam (*viz.* line-of-sight to observer).

6.3. PSR J2019+2425

PSR J2019+2425 is a BMSP with $P_{\rm orb} = 76.5$ days and a mass function $f = 0.0107 M_\odot$ (Nice et al. 1993). In a recent paper (Tauris 1998) it was demonstrated that for this pulsar $M_{\rm NS} \simeq 1.20\,M_\odot$, if the $(P_{\rm orb}, M_{\rm WD})$ correlation obtained by Rappaport et al. (1995) was taken at face value. This

value of $M_{\rm NS}$ is significantly lower than that of any other estimated pulsar mass (Thorsett & Chakrabarty 1999). However with the new ($P_{\rm orb}, M_{\rm WD}$) correlation presented in this paper we obtain a larger maximum mass ($i = 90°$) of this pulsar: $M_{\rm NS}^{\rm max} = 1.39\,M_\odot$ or $1.64\,M_\odot$ for a donor star of Pop.I or Pop.II chemical composition, respectively. This result brings the mass of PSR J2019+2425 inside the interval of typical estimated values of $M_{\rm NS}$.

6.4. $M_{\rm NS}$: dependence on the propeller effect and accretion disk instabilities

It is still an open question whether or not a significant amount of mass can be ejected from an accretion disk as a result of the effects of disk instabilities (Pringle 1981; van Paradijs 1996). However, there is clear evidence from observations of Be/X-ray transients that a strong braking torque acts on these neutron stars which spin near their equilibrium periods. The hindering of accretion onto these neutron stars is thought to be caused by their strong rotating magnetic fields which eject the incoming material via centrifugal acceleration – the so-called propeller effect (Illarionov & Sunyaev 1985).

For a given observed BMSP we know $P_{\rm orb}$ and using Eqs. (20), (21) we can find $M_{\rm WD}$ for an adopted chemical composition of the donor star. Hence we are also able to calculate the maximum gravitational mass of the pulsar, $M_{\rm NS}^{\rm max}$ (which is found for $i = 90°$, cf. Eq. 23) since we know the mass function, f from observations. This semi-observational constraint on $M_{\rm NS}^{\rm max}$ can then be compared with our calculations of $M'_{\rm NS}$ (cf. Sect. 5.7). The interesting cases are those where $M'_{\rm NS} > M_{\rm NS}^{\rm max}$ (after correcting $M'_{\rm NS}$ for the mass deficit). These systems *must* therefore have lost matter ($\Delta M_{\rm dp} \neq 0$), from the accretion disk or as a result of the propeller effect, in addition to what is ejected when $|\dot{M}_2| > \dot{M}_{\rm Edd}$. These binaries are plotted in Fig. 4b assuming an 'intermediate' Pop. I+II chemical composition for the progenitor of the white dwarf. We notice that in a some cases we must require $\Delta M_{\rm dp} \simeq 0.50\,M_\odot$, or even more for $M_2 > 1.0\,M_\odot$, in order to get $M_{\rm NS}$ below the maximum limit ($M_{\rm NS}^{\rm max}$) indicated by the plotted arrow. We therefore conclude that mass ejection, in addition to what is caused by super-Eddington mass-transfer rates, is very important in LMXBs. Whether or not this conclusion is equally valid for super- and sub-Eddington accreting systems is difficult to answer since systems which evolve through an X-ray phase with super-Eddington mass-transfer rates lose a large amount of matter from the system anyway and therefore naturally end up with small values of $M'_{\rm NS}$.

6.5. Kaon condensation and the maximum mass of NS

It has recently been demonstrated (Brown & Bethe 1994; Bethe & Brown 1995) that the introduction of kaon condensation sufficiently softens the equation-of-state of dense matter, so that NS with masses more than $\sim 1.56\,M_\odot$ will not be stable and collapse into a black hole. If this scenario is correct, then we expect a substantial fraction of LMXBs to evolve into black hole binaries – unless $\Delta M_{\rm dp}$ is comparable to the difference between M_2 and $M_{\rm WD}$ as indicated above. However, it has recently been reported by Barziv et al. (1999) that the HMXB Vela X-1 has a minimum value for the mass of the neutron star of $M_{\rm NS} > 1.68\,M_\odot$ at the 99 % confidence level. It is therefore still uncertain at what critical mass the NS is expected to collapse into a black hole.

6.6. PSR J1603–7202

The maximum allowed value of the pulsar mass in this system is extremely low compared to other BMSP systems with He-WD companions. We find $M_{\rm NS}^{\rm max} = 0.96$–$1.11\,M_\odot$ depending on the chemical abundances of the white dwarf progenitor. It is therefore quite suggestive that this system did not evolve like the other BMSPs with a He-WD companion. Furthermore (as noted by Lorimer et al. 1996), it has a relatively slow spin period of $P_{\rm spin} = 14.8$ ms and $P_{\rm orb} = 6.3$ days. Also its location in the (P,$\dot{P}$) diagram is atypical for a BMSP with a He-WD (Arzoumanian et al. 1999). All these characteristica are in common with BMSPs which possibly evolved through a CE evolution (van den Heuvel 1994b; Camilo 1996). We conclude therefore, that this system evolved through a phase with critical unstable mass-transfer (like in a CE) and hence most likely hosts a CO-WD companion rather than a He-WD companion. The latter depends on whether or not helium core burning was ignited, and thus on the value of $P_{\rm orb}^{\rm i}$ and M_2. Spectroscopic observations should answer this question.

7. Conclusions

- We have adapted a numerical computer code, based on Eggleton's code for stellar evolution, in order to carefully study the details of mass-transfer in LMXB systems. We have included, for the first time to our knowledge, other tidal spin-orbit couplings than magnetic braking and also considered wind mass-loss during the red giant stage of the donor star.
- We have re-calculated the ($P_{\rm orb}, M_{\rm WD}$) correlation for binary radio pulsar systems using new input physics of stellar evolution in combination with detailed binary interactions. We find a correlation which yields a larger value of $M_{\rm WD}$ for a given value of $P_{\rm orb}$ compared to previous work.
- Comparison between observations of BMSPs and our calculated post-accretion $M_{\rm NS}$ suggests that a large amount of matter is lost from the LMXBs; probably as a result of either accretion disk instabilities or the propeller effect. Hence it is doubtful whether or not observations will reveal an ($P_{\rm orb}, M_{\rm NS}$) anti-correlation which would otherwise be expected from our calculations.
- The mass-transfer rate is a strongly increasing function of initial orbital period and donor star mass. For relatively close systems with light donors ($P_{\rm orb}^{\rm ZAMS} < 10$ days and $M_2 < 1.3\,M_\odot$) the mass-transfer rate is sub-Eddington, whereas it can be highly super-Eddington by a factor of $\sim 10^4$ for wide systems with relatively heavy donor stars ($1.6 \sim 2.0\,M_\odot$),

as a result of their deep convective envelopes. Binaries with (sub)giant donor stars with mass in excess of $\sim 2.0\,M_\odot$ are unstable to dynamical timescale mass loss. Such systems will evolve through a common envelope evolution leading to a short (< 10 days) orbital period BMSP with a heavy CO/O-Ne-Mg white dwarf companion. Binaries with unevolved heavy ($> 2\,M_\odot$) donor stars might be dynamically stable against a CE, but also end up with a relatively short $P_{\rm orb}$ and a CO/O-Ne-Mg WD.

– Based on our calculations, we present new evidence that PSR J1603–7202 did not evolve through a phase with stable mass transfer and that it is most likely to have a CO white dwarf companion.
– The pulsar mass of PSR J2019+2425 now fits within the standard range of measured values for $M_{\rm NS}$, given our new ($P_{\rm orb}, M_{\rm WD}$) correlation.

Acknowledgements. We would like to thank Ed van den Heuvel for several discussions on many issues; Guillaume Dubus for discussions on accretion disk instabilities; Jørgen Christensen-Dalsgaard for pointing out the well-known tiny loop in the evolutionary tracks of low-mass stars on the RGB and Lev Yungelson for comments on the manuscript. T.M.T. acknowledges the receipt of a Marie Curie Research Grant from the European Commission.

Appendix A: Tidal torque and dissipation rate

We estimate the tidal torque due to the interaction between the tidally induced flow and the convective motions in the stellar envelope by means of the simple mixing-length model for turbulent viscosity $\nu = \alpha H_{\rm p} V_{\rm c}$, where the mixing-length parameter α is adopted to be 2 or 3, $H_{\rm p}$ is the local pressure scaleheight, and $V_{\rm c}$ the local characteristic convective velocity. The rate of tidal energy dissipation can be expressed as (Terquem et al. 1998):

$$\frac{{\rm d}E}{{\rm d}t} = -\frac{192\pi}{5}\Omega^2 \int_{R_i}^{R_o} \rho r^2 \nu \left[\left(\frac{\partial \xi_r}{\partial r} \right)^2 + 6 \left(\frac{\partial \xi_h}{\partial r} \right)^2 \right] dr \quad \text{(A1)}$$

where the integration is over the convective envelope and Ω is the orbital angular velocity, i.e. we neglect effects of stellar rotation. The radial and horizontal tidal displacements are approximated here by the values for the adiabatic equilibrium tide:

$$\xi_r = f r^2 \rho \left(\frac{{\rm d}P}{{\rm d}r} \right)^{-1} \quad \text{(A2)}$$

$$\xi_h = \frac{1}{6r} \frac{{\rm d}(r^2 \xi_r)}{{\rm d}r} \quad \text{(A3)}$$

where for the dominant quadrupole tide ($l = m = 2$) $f = \frac{-GM_2}{4a^3}$.

The locally dissipated tidal energy is taken into account as an extra energy source in the standard energy balance equation of the star, while the corresponding tidal torque follows as:

$$\Gamma = -\frac{1}{\Omega} \frac{{\rm d}E}{{\rm d}t} \quad \text{(A4)}$$

The thus calculated tidal angular momentum exchange $dJ = \Gamma dt$ between the donor star and the orbit during an evolutionary timestep dt is taken into account in the angular momentum balance of the system. If the so calculated angular momentum exchange is larger than the amount required to keep the donor star synchronous with the orbital motion of the compact star we adopt a smaller tidal angular momentum exchange (and corresponding tidal dissipation rate in the donor star) that keeps the donor star exactly synchronous.

References

Alberts F., Savonije G.J., van den Heuvel E.P.J., Pols O.R., 1996, Nat 380, 676
Arzoumanian Z., Cordes J.M., Wasserman I., 1999, ApJ 520, 696
Barziv O., Kaper L., van Kerkwijk M.H., Telting J.H., van Paradijs J.A., 1999, in preparation
Bethe H.A., Brown G.E., 1995, ApJ 445, L129
Bhattacharya D., van den Heuvel E.P.J., 1991, Phys. Reports 203, 1
Brown G.E., Bethe H.A., 1994, ApJ 423, 659
Brown G.E., 1995, ApJ 440, 270
Camilo F., 1995, Ph.D. Thesis, Princeton University
Camilo F., 1996, In: Johnston S., Walker M.A., Bailes M. (eds.) Pulsars: Problems and Progress. ASP Conf. Series Vol. 105, p. 539
Chevalier R.A., 1993, ApJ 411, L33
Chevalier R.A., 1996, ApJ 459, 332
Eggleton P.P., 1983, ApJ 268, 368
Ergma E., Sarna M.J., Antipova J., 1998, MNRAS 300, 352
Han Z., Podsiadlowski P., Eggleton P.P, 1994, MNRAS 270, 121
Hansen B.M.S., Phinney E.S., 1998, MNRAS 294, 569
Hjellming M.S., Webbink R.F., 1987, ApJ 318, 794
Hjellming M.S., 1989, Ph.D. Thesis, University of Illinois
Iben Jr., Livio M., 1993, PASP 105, 1373
Illarionov A.F., Sunyaev R.A., 1985, A&A 39, 185
Joss P.C., Rappaport S.A., Lewis W., 1987, ApJ 319, 180
Kalogera V., Webbink R.F., 1996, ApJ 458, 301
Kippenhahn R., Weigert A., 1990, Stellar Structure and Evolution. A&A Library, Springer-Verlag
Landau L.D., Lifshitz E., 1958, The Classical Theory of Fields. Pergamon Press, Oxford
Lorimer D.R., Lyne A.G., Bailes M., et al., 1996, MNRAS 283, 1383
Nice D.J., Taylor J.H., Fruchter A.S., 1993, ApJ 402, L49
Paczynski B., 1976, In: Eggleton P.P., Mitton S., Whealan J. (eds.) Structure and Evolution in Close Binary Systems. Proc. IAU Symp.73, Reidel, Dordrecht, p. 75
Parker E.N., 1955, ApJ 121, 491
Phinney E.S., Kulkarni S.R., 1994, ARA&A 32, 591
Podsiadlowski P., 1991, Nat 350, 136
Pols O.R., Tout C.A., Eggleton P.P., Han Z., 1995, MNRAS 274, 964
Pols O.R., Schröder K.P., Hurley J.R., Tout C.A., Eggleton P.P., 1998, MNRAS 298, 525
Pringle J.E., 1981, ARA&A 19, 137
Pylyser E., Savonije G.J., 1988, A&A 191, 57
Pylyser E., Savonije G.J., 1989, A&A 208, 52
Rappaport S.A., Verbunt F., Joss P.C., 1983, ApJ 275, 713
Rappaport S.A., Podsiadlowski P., Joss P.C., Di Stefano R., Han Z., 1995, MNRAS 273, 731
Refsdal S., Weigert A., 1971, A&A 13, 367
Reimers D., 1975, In: Bascheck B., Kegel W.H., Traving G. (eds.) Problems in Stellar Atmospheres and Envelopes. Springer, New York, p. 229
Renzini A., 1981, In: Chiosi C., Stalio R. (eds.) Effects of Mass Loss on Stellar Evolution. Reidel, Dordrecht, p. 319
Sackmann I.-J., Boothroyd A.I., Kraemer K.E., 1993, ApJ 418, 457

Table A1. LMXB systems calculated for the work presented in this paper. Pop. I and Pop. II chemical compositions correspond to X=0.70, Z=0.02 and X=0.75, Z=0.001, respectively. α is the mixing-length parameter. $P_{\rm orb}$ is in units of days and the masses are in units of $M_\odot$.

$M_2 = 1.0$		$\alpha = 2.0$		Pop. I	
$P_{\rm orb}^{\rm ZAMS}$	$P_{\rm orb}^{\rm RLO}$	$P_{\rm orb}^{\rm f}$	$M_{\rm WD}^{\rm theo}$	$M'_{\rm NS}$	$t_{\rm X}$
2.6	0.64	0.09	0.133	2.17	–
2.7	0.72	1.28	0.190	2.11	2790
2.8	0.81	4.08	0.221	2.08	1740
2.9	0.94	7.24	0.236	2.06	1240
3.0	1.04	9.98	0.245	2.06	990
3.4	1.48	18.8	0.264	2.03	613
4.0	2.32	30.9	0.280	2.02	350
5.0	4.0	47.1	0.294	2.00	190
6.0	5.2	57.0	0.302	1.99	145
10.0	9.2	88.0	0.318	1.93	72.0
15.0	14.1	121.9	0.332	1.85	46.3
25.0	23.7	187.6	0.353	1.69	28.5
40.0	38.4	277.9	0.374	1.58	18.5
60.0	58.1	381.9	0.395	1.49	13.3
100	98.3	554.4	0.423	1.42	8.6
150	150	727.8	0.449	1.39	6.2
200	204	873.4	0.469*	1.37	6.1
300	315	1104.0	0.500*	1.35	3.5
400	433	1266.5	0.528*	1.34	2.4
600	692	1349.0	0.596*	1.32	1.1
800	982	1285.6	0.668*	1.30	0.4

$M_2 = 1.0$		$\alpha = 2.0$		Pop. II	
$P_{\rm orb}^{\rm ZAMS}$	$P_{\rm orb}^{\rm RLO}$	$P_{\rm orb}^{\rm f}$	$M_{\rm WD}^{\rm theo}$	$M'_{\rm NS}$	$t_{\rm X}$
3.0	0.73	0.56	0.195	2.11	3090
3.1	0.82	3.16	0.235	2.06	1570
3.2	0.94	6.25	0.256	2.04	1110
3.4	1.26	11.9	0.277	2.02	770
4.0	2.12	23.4	0.300	2.00	430
5.0	4.0	38.3	0.318	1.98	220
6.0	5.2	46.6	0.326	1.97	174
8.0	7.3	59.9	0.337	1.95	140
10.0	9.2	71.9	0.344	1.93	85.0
15.0	14.1	99.5	0.358	1.85	54.0
25.0	23.8	151.8	0.379	1.72	32.3
40.0	38.5	226.3	0.402	1.59	21.1
60.0	58.5	314.2	0.423	1.51	14.7
80.0	78.7	392.3	0.439	1.46	11.6
100	99.3	462.3	0.452	1.44	9.5
150	152	613.0	0.478*	1.40	6.7
200	207	740.9	0.498*	1.38	5.3

$M_2 = 1.0$		$\alpha = 3.0$		Pop. I	
$P_{\rm orb}^{\rm ZAMS}$	$P_{\rm orb}^{\rm RLO}$	$P_{\rm orb}^{\rm f}$	$M_{\rm WD}^{\rm theo}$	$M'_{\rm NS}$	$t_{\rm X}$
2.5	0.59	0.36	0.168	2.13	4400
2.6	0.68	2.28	0.212	2.09	1980
2.7	0.80	5.63	0.237	2.06	1180
2.8	0.94	8.38	0.248	2.05	930
2.9	1.06	10.9	0.257	2.04	730
3.0	1.17	12.8	0.262	2.04	645
3.4	1.60	20.6	0.278	2.02	400
4.0	2.87	33.0	0.296	2.00	212
5.0	4.2	44.0	0.307	1.99	138
6.0	5.3	52.3	0.314	1.97	106
8.0	7.3	66.3	0.325	1.94	68.4
10.0	9.2	79.7	0.333	1.88	51.5
15.0	14.1	111.7	0.349	1.76	34.2
25.0	23.7	173.0	0.373	1.60	21.0
40.0	38.4	252.5	0.396	1.50	13.6
60.0	58.2	342.7	0.418	1.44	9.5
80.0	78.6	420.0	0.434	1.41	7.5
100	99.0	489.2	0.449	1.39	6.3
150	151	635.7	0.476*	1.37	4.4
200	206	756.4	0.499*	1.35	3.4

$M_2 = 1.3$		$\alpha = 2.0$		Pop. I	
$P_{\rm orb}^{\rm ZAMS}$	$P_{\rm orb}^{\rm RLO}$	$P_{\rm orb}^{\rm f}$	$M_{\rm WD}^{\rm theo}$	$M'_{\rm NS}$	$t_{\rm X}$
2.3	0.79	0.016	0.144	2.44	–
2.35	0.84	2.30	0.208	2.39	2590
2.4	0.96	5.53	0.229	2.37	1720
2.5	1.08	9.66	0.244	2.36	1140
2.6	1.13	12.8	0.252	2.35	900
2.7	1.17	15.3	0.257	2.32	790
2.8	1.23	16.9	0.261	2.28	725
2.9	1.28	19.0	0.264	2.26	665
3.0	1.35	21.0	0.267	2.24	610
3.4	1.61	27.9	0.276	2.22	444
4.0	2.02	36.6	0.285	2.25	366
5.0	3.63	58.5	0.303	2.20	190
6.0	4.89	73.3	0.311	2.14	133
10.0	8.85	113.5	0.329	2.14	74.0
15.0	13.6	162.9	0.346	1.85	40.0
25.0	22.9	253.1	0.370	1.65	22.6
40.0	37.2	369.6	0.393	1.54	16.4
60.0	56.4	500.5	0.416	1.47	11.5
100	95.4	714.6	0.448	1.41	7.6
150	146	933.5	0.478*	1.38	5.4
200	197	1108.8	0.502*	1.36	4.4

$M_2 = 1.6$		$\alpha = 2.0$		Pop. I	
$P_{\rm orb}^{\rm ZAMS}$	$P_{\rm orb}^{\rm RLO}$	$P_{\rm orb}^{\rm f}$	$M_{\rm WD}^{\rm theo}$	$M'_{\rm NS}$	$t_{\rm X}$
1.5	1.09	0.08	0.147	2.75	–
1.8	1.15	1.20	0.189	2.71	2350
2.0	1.20	6.05	0.219	2.68	780
2.1	1.27	11.2	0.246	2.65	450
2.2	1.30	19.6	0.263	2.63	285
2.6	1.68	33.6	0.283	2.13	136
3.0	2.00	41.8	0.291	2.05	123
4.0	2.90	58.0	0.303	2.06	107
6.0	5.0	87.1	0.320	2.04	78.0
8.0	6.8	109.6	0.330	2.00	61.0
10.0	8.7	133.4	0.339	1.85	42.0
15.0	13.3	194.7	0.358	1.62	23.2
25.0	22.3	309.2	0.384	1.50	14.5
40.0	36.0	451.5	0.410	1.44	9.3
60.0	54.5	608.0	0.435	1.40	7.5
100	92.3	828.9	0.466*	1.37	5.1
150	141	1035.1	0.494*	1.36	4.1
200	190	1192.8	0.531*	1.35	3.2

$M_2 = 2.0$		$\alpha = 2.0$		Pop. I	
$P_{\rm orb}^{\rm ZAMS}$	$P_{\rm orb}^{\rm RLO}$	$P_{\rm orb}^{\rm f}$	$M_{\rm WD}^{\rm theo}$	$M'_{\rm NS}$	$t_{\rm X}$
1.2	1.19	0.05	0.117	2.84	–
1.3	1.29	2.82	0.211	2.75	1820
1.4	1.39	5.82	0.232	2.75	1070
1.5	1.49	9.56	0.247	2.75	650
1.6	1.59	14.9	0.259	2.76	410
1.7	1.69	22.7	0.269	2.76	218
1.75	1.74	8.1	0.278	2.74	160
1.77	1.76	0.5	0.281	2.72	124
1.79	1.78	4.1	0.289	2.55	100
1.8	1.79	38.6	0.297	1.83	49.0
1.9	1.89	39.7	0.301	1.82	37.8
2.0	2.00	41.0	0.305	1.81	37.0
2.2	2.20	44.6	0.310	1.79	37.0
2.4	2.40	48.2	0.313	1.76	36.0
2.6	2.60	51.6	0.316	1.74	34.2
2.8	2.78	54.7	0.318	1.71	32.8
3.0	2.89	56.2	0.320	1.64	28.5
3.2	2.76	56.4	0.320	1.57	24.0
3.4	2.94	59.7	0.322	1.57	24.0
3.6	3.15	63.3	0.324	1.57	23.8
3.8	3.37	66.7	0.326	1.57	24.1
4.0	3.58	69.8	0.327	1.57	24.2
4.2	3.79	73.0	0.328	1.57	24.0
>4.2		–	–	–	–

* This is the mass of M_2 when the $\sim 0.47\,M_\odot$ He-core ignites (flash).
$P_{\rm orb}^{\rm ZAMS}$ is the initial orbital period of the NS and the unevolved companion.
$P_{\rm orb}^{\rm RLO}$ is the orbital period at onset of RLO.
$P_{\rm orb}^{\rm f}$ is the final orbital period of the LMXB – or the (initial) period of the BMSP.
$M_{\rm WD}^{\rm theo}$ is our calculated mass of the helium WD.
$M'_{\rm NS}$ is the final mass of the NS if $\Delta M_{\rm dp} = 0$.
$t_{\rm X}$ is the integrated duration time (Myr) that the binary is an *active* X-ray source.

Table A2. Observed binary pulsars (NS+WD) in the Galactic disk. Masses are in units of $M_\odot$.

PSR	$P_{\rm orb}$ (days)	f ($M_\odot$)	$M_{\rm WD}^{\rm obs}$	$M_{\rm WD}^{\rm theo}$	$i^{\rm theo}$ (deg.)	$M_{\rm NS}^{\rm max}$	$M'_{\rm NS}$	$P_{\rm spin}$ (ms)	Class
B0820+02	1232	0.003	0.231	0.503	26.1	6.02	1.34	865	A*
J1803–2712	407	0.0013	0.170	0.423	22.7	7.20	1.48	334	A
J1640+2224	175	0.0058	0.295	0.373	44.9	2.61	1.69	3.16	A
J1643–1224	147	0.00078	0.142	0.363	21.7	7.48	1.82	4.62	A
B1953+29	117	0.0024	0.213	0.352	33.6	3.90	1.86	6.13	A
J2229+2643	93.0	0.00084	0.146	0.340	23.7	6.51	1.90	2.98	A
J2019+2425	76.5	0.0107	0.373	0.331	73.5	1.51	1.93	3.93	A
J1455–3330	76.2	0.0063	0.304	0.331	53.5	2.07	1.93	7.99	A
J1713+0447	67.8	0.0079	0.332	0.326	61.6	1.77	1.95	4.57	A
J2033+1734	56.2	0.0027	0.222	0.318	38.9	3.13	1.97	5.94	A
B1855+09	12.33	0.00557	0.291	0.262	71.5	1.54	2.05	5.36	AB
J1804–2717	11.13	0.00335	0.241	0.259	54.0	2.02	2.05	9.34	AB
J0621+1002	8.319	0.0271	0.540	0.251	>90	0.51	2.06	28.9	C
J1022+1001	7.805	0.0833	0.872	0.249	>90	0.18	2.06	16.5	C
J2145–0750	6.839	0.0242	0.515	0.245	>90	0.54	2.07	16.1	C
J2129–5721	6.625	0.00105	0.158	0.244	35.4	3.48	2.07	3.73	AB
J1603–7202	6.309	0.00881	0.346	0.243	>90	1.03	2.07	14.8	C
J0437–4715	5.741	0.00125	0.168	0.240	38.5	3.09	2.08	5.76	AB
J1045–4509	4.084	0.00177	0.191	0.232	46.4	2.42	2.09	7.45	AB
J1911–1114	2.717	0.000799	0.143	0.222	35.2	3.48	2.09	3.63	B
J2317+1439	2.459	0.00221	0.206	0.220	54.8	1.97	2.10	3.44	B
J0218+4232	2.029	0.00204	0.201	0.216	54.1	2.00	2.10	2.32	B
B1831–00	1.811	0.000124	0.075	0.213	18.8	8.64	2.10	521	B
J0034–0534	1.589	0.00127	0.169	0.211	45.0	2.50	2.11	1.88	B
J0613–0200	1.119	0.000972	0.154	0.205	41.5	2.78	2.12	3.06	B
B0655+64	1.029	0.0714	0.814	0.202	>90	0.14	2.12	196	C
J1012+5307	0.605	0.000580	0.128	0.193	36.1	3.33	2.13	5.26	B
B1957+20	0.382	0.0000052	0.026	0.186	7.3	35.0	2.15	1.61	B
J0751+1807	0.263	0.000974	0.154	0.181	48.2	2.28	2.16	3.48	B
J2051–0827	0.099	0.000010	0.032	0.168	10.0	21.7	2.18	4.51	B

The last column gives the classification of the BMSPs. Class A represents the wide-orbit binaries with He-WD companions. Class B contains the close-orbit binaries with He-WD companions. In these class B systems non-conservative angular momentum losses ($\dot{J}_{\rm gwr}$, $\dot{J}_{\rm mb}$ and irradiation) were dominant in the evolution of the progenitor LMXB and $P_{\rm orb}^{\rm i} < P_{\rm bif}$. The subclass AB refers to systems in which tidal spin-orbit interactions were important but not sufficiently strong to finally prevent the orbit from widening ($P_{\rm orb}^{\rm i} \approx$ 2–3 days). Class C hosts the BMSPs with heavy CO-WD companions. These systems evolved through (and survived) a phase with extreme mass-transfer rates and loss of orbital angular momentum (e.g. a common envelope).

$M_{\rm WD}^{\rm obs}$ is the mass of the white dwarf assuming $i = 60^\circ$ (the mean value of a random isotropic distribution) and $M_{\rm NS} = 1.4\,M_\odot$.
$M_{\rm WD}^{\rm theo}$ is the mass of the white dwarf obtained from our ($P_{\rm orb}, M_{\rm WD}$) correlation assuming a Pop. I+II composition for the donor.
$i^{\rm theo}$ is the orbital inclination angle required for $M_{\rm WD}^{\rm obs} = M_{\rm WD}^{\rm theo}$; $i > 90^\circ$ means there is no solution (the observed WD is 'too heavy').
$M_{\rm NS}^{\rm max}$ is the maximum value for $M_{\rm NS}$ obtained from the observed binary mass function, f using $i = 90^\circ$ and $M_{\rm WD} = M_{\rm WD}^{\rm theo}$.
$M'_{\rm NS}$ is a rough estimate of the potential maximum post-accretion mass of the NS assuming $\Delta M_{\rm dp} = 0$ (see curves in Fig. 4b).
For references to the observed values ($P_{\rm orb}$, f and $P_{\rm spin}$) see e.g. Camilo (1995) and Lorimer et al (1996).
* The companion of this very wide-orbit pulsar might be a CO white dwarf (cf. Sect. 6.2).

Savonije G.J., 1987, Nat 325, 416
Shapiro S.L., Teukolsky S.A., 1983, Black Holes, White Dwarfs and Neutron Stars. Wiley-Interscience
Skumanich A., 1972, ApJ 171, 565
Soberman G.E., Phinney E.S., van den Heuvel E.P.J., 1997, A&A 327, 620
Taam R.E., 1983, ApJ 270, 694
Tauris T.M., 1996, A&A 315, 453
Tauris T.M., 1998, A&A 334, L17
Tavani M., 1992, In: van den Heuvel E.P.J., Rappaport S.A. (eds.) X-ray Binaries and Recycled Pulsars. Kluwer, Dordrecht, p. 387
Terquem C., Papaloizou J.C.B., Nelson R.P., Lin D.N.C, 1998, ApJ 502, 788
Thomas H.C., 1967, Z. Astrophys. 67, 420
Thorsett S.E., Chakrabarty D., 1999, ApJ 512, 288
van den Heuvel E.P.J., 1975, ApJ 198, L109
van den Heuvel E.P.J., 1994a, In: Nussbaumer H., Orr A. (eds.) Interacting Binaries. Saas-Fee 1992 lecture notes, Springer-Verlag
van den Heuvel E.P.J., 1994b, A&A 291, L39
van Paradijs J., 1996, ApJ 464, L139
Verbunt F., 1990, In: Kundt W. (ed.) Neutron Stars and Their Birth Events. Kluwer, Dordrecht, p. 179
Verbunt F., Zwaan C., 1981, A&A 100, L7
Verbunt F., Phinney E.S., 1995, A&A 296, 709
Webbink R.F., 1984, ApJ 277, 355
Webbink R.F., Rappaport S.A., Savonije G.J., 1983, ApJ 270, 678